Molecular Mechanism of Al Inducible Malate Excretion of *Arabidopsis thaliana*

(シロイヌナズナのアルミニウム誘導性リンゴ酸放出の分子機構)

2018

The United Graduate School of Agricultural Science,

Gifu University

Science of Biological Resources

(Gifu University)

WU LIUJIE

Molecular Mechanism of Al Inducible Malate Excretion of *Arabidopsis thaliana*

(シロイヌナズナのアルミニウム誘導性リンゴ酸放出の分子機構)

WU LIUJIE

CONTENTS

I

Screening of Chemical Compounds that Reduced Malate Secretion in *Arabidopsis thaliana*

ABSTRACT

Arabidopsis thaliana protects its sensitive root tips from aluminum toxicity by activating malate secretion through aluminum-activated malate transporter 1 (ALMT1), which is regulated by gene expression and malate transport activity. In this study, we used a library of specific inhibitors to discovery novel factors involved in Al-responsive AtALMT1 signaling pathway. This library consisted over 200 specific inhibitors of various protein kinases/phosphatases and inositol-related kinases, which are frequently used for profiling signal transduction pathways in medical researches. From the screening, three inhibitors (PIK-75, AZD7762, and WP1130) were identified as differently affected Al-inducible malate secretion. We found that AZD7762 affected Al-induced *AtALMT1* expression in the late phase of treatment, while WP1130 inactivated malate transport activity. On the other hand, PIK-75 inhibited both early Al-inducible *AtALMT1* expression and malate transport activity. Furthermore, Al-inducible expression of all the tested genes (e.g. STOP1-regulated genes and Al-biomarker genes) was significantly suppressed by PIK-75. These results suggest that PIK-75 inhibited an essential and common process of early Al-responsive signal transduction pathway.

1. INTRODUCTION

Aluminum (Al^{3+}) toxicity is one of the major limiting factors affecting plant production in acidic soils. The primary symptom of Al toxicity is inhibitory root growth. For instance, the rapid inhibition (within 1 h) of root growth primarily caused by a block in cell elongation, while a long-time exposure to Al (>24 h) both cell elongation and division are blocked (Jones et al., 1995; Kochian, 1995). Believably, plant species have evolved lots of mechanisms for adapting to the acidic soil environment. These mechanisms could be divided into two distinct categories of Al resistance: resistance (exclusion) mechanisms and tolerance mechanisms. Firstly, exclusion of organic acids (OAs), such as malate and citrate, into the rhizosphere can detoxify Al toxicity by chelating the free Al^{3+} to Al-OAs complexes (Ryan et al., 1995) and enhance defense mechanisms through induced systemic resistance by recruiting beneficial rhizobacteria (Rudrappa et al., 2008). Secondly, tolerance mechanisms, which enable plants to hold Al safely once it enters the symplast, include chelating the intracellular Al^{3+} to form the harmless complexes and store Al^{3+} in subcellular compartments that harmless for plants. Currently, our knowledge of Al resistance in some crop plants has increased dramatically, due to the application of genetics and molecular biology. However, with population growth and climate change, the demand for food will rapidly increase. To address this urgent problem, transgenic strategies would be a beneficial way to develop high tolerance crop plants against Al stress (Hoisington, 2002; Bhalla, 2006).

Al-induced malate secretion in Arabidopsis would be a good model to use to clarify the molecular mechanisms of OA secretion. Malate secretion is regulated by both Al-inducible expression of *AtALMT1* and Al-activated malate transport by AtALMT1 (Daspute et al., 2018). The former is controlled by both quick (e.g. <3 h) and inducible (e.g. 24 h) processes using various transcription factors. For example, sensitive to proton rhizotoxicity 1 (STOP1; Iuchi et

al., 2007) is essential for a quick Al-responsive expression of *AtALMT1*, while transcription of *CAMTA2* (*AtALMT1* activator; Tokizawa et al., 2015) and *WRKY46* (*AtALMT1* repressor; Ding et al., 2013) regulates the inducible expression of *AtALMT1*. By contrast, the activation of AtALMT1, a malate transporter, is directly regulated by the Al binding to the protein and by post-translational regulation (Sasaki et al., 2004; Kobayashi et al., 2007; Ligaba et al., 2009). From these findings, we can infer that other molecules involve in the regulatory mechanisms of each process. Part of this complex mechanism can be from various molecules that induce *AtALMT1* expression, such as phytohormones (e.g. IAA and ABA) and hydrogen peroxide (Kobayashi et al., 2013a). The gene is also induced by biotic stimuli, such as the FLG22-peptide of microbe-associated molecular patterns (Lakshmanan et al., 2012; Kobayashi et al., 2013a), and typical pathogen signaling pathways regulated by coronatine insensitive 1 and jasmonic acid (Yang et al., 2017). These complex regulations could account for the pleiotropic roles of AtALMT1-dependent malate secretion in stress tolerance. Further studies are necessary to clarify the complex regulating mechanisms of AtALMT1, which is associated with various beneficial phenotypes.

An electrostatics study, which assessed Al^{3+} activity at the plasma membrane (PM) surface ($\{Al^{3+}\}_{PM}$), revealed that the activation of *AtALMT1* expression and several other Al-biomarker genes are very sensitive to Al (Kobayashi et al., 2013b). Association of $\{Al^{3+}\}_{PM}$ and Al-inducible expression of several genes suggested Al-sensing mechanisms of the PM. In contrast, STOP1 coregulates Al-inducible expression of *AtALMT1* and other Al-tolerance genes, namely *ALUMINUM SENSITIVE 3* (*ALS3*) and *multidrug and toxic compound extrusion* (*MATE*) (Sawaki et al., 2009), while it does not regulate the expression of the above Al-biomarker genes (Kobayashi et al., 2013b). These findings suggest a common Al-sensing process that activates the transcription of several genes but that might be regulated differently by distinct signal

transducers, which are regulated post-translationally (e.g. protein phosphorylation). In fact, previous studies identified that Al signaling is blocked by protein kinase inhibitors. For example, K-252a blocks malate secretion in wheat (Osawa and Matsumoto, 2001) and Arabidopsis (Kobayashi et al., 2007), while several other inhibitors suppress citrate-transporting *MATE* in eucalypts, which is an Al-inducible expression regulated by STOP1-like protein (Sawaki et al., 2013).

Another factor that controls malate secretion is Al-activation of ALMT1 protein, which occurs in a quick manner. A wheat study identified that extracellular Al^{3+} might activate TaALMT1 by binding to negatively charged amino acids of the ALMT1 domain that localized at extracellular space (Sasaki et al., 2014). However, Al-activated malate secretion by AtALMT1 was immediately stopped by removing Al from the incubating solutions; while it was maintained by the addition of protein phosphatase inhibitor Cyclosporin A (Kobayashi et al., 2007). Additionally, Ligaba et al. (2009) found that the malate transporter TaALMT1 is affected by mutations at the phosphorylation sites within the protein. Taken all, these results suggest that the malate transporters directly interact with Al^{3+} and its post-translational mechanisms involve protein phosphorylation that regulates malate transport by ALMT1.

The pharmacological approach, which uses small molecules to rapidly and conditionally inactivate proteins, is one approach to studying molecular mechanisms (Ellman, 1996; Thompson and Ellman, 1996; Alaimo et al., 2001). In medical studies, small-molecule compounds that show nearly target-specific behavior to proteins have been used to study complex biological processes, which include changes in the signal transduction in cancer and tumor cells. A similar approach would be useful for studying complex regulatory mechanisms of such as Al-induced OA secretion. In fact, this approach has been used to identify several small molecules that affect signal transductions in plants (Brown et al., 2011; Nishimura et al.,

2014). Recently, a small molecule 3-amino-N-(3-methyl phenyl)thieno[2,3-b]pyridine-2-carboxamide, screened from a library of 5000 compounds, was found to target the FIT-dependent transcriptional pathway in Arabidopsis under iron deficiency stress (Kailasam et al., 2018). In the current study, we used this approach to identify unknown regulators of Al-inducible malate secretion. We used a library of more than 200 inhibitors, mainly protein kinase inhibitors that have been used in human pharmacological research for discovering cancer-related drugs. The library also included inhibitors that suppress early signal transduction in cancer responses, such as those for signaling lipids. Some of these processes have been proposed as an early Al-signaling mechanism (e.g. phospholipid signaling; Jones and Kochian, 1995; Jones and Kochian, 1997; Martínez-Estévez et al., 2003), while their relationship to OA secretion has not been clarified.

2. MATERIALS AND METHODS

Arabidopsis accessions

Arabidopsis thaliana wild-type Col-0 (Columbia) was obtained from the RIKEN BioResource Center. A transgenic Arabidopsis that overexpressed *AtALMT1* using the cauliflower mosaic virus 35S promoter (35S:*AtALMT1*) was developed by Kobayashi et al. (2013a) using Col-0 as the host. In this study, the homozygous T_3 generation of 35S:*AtALMT1* was used to analyze the suppression effects of inhibitors on Al-activated malate transport by AtALMT1. Transgenic Arabidopsis that STOP1 fused to a *GFP* gene driven by the AtSTOP1 promoter (*ProSTOP1:STOP1-GFP*) were obtained from the RIKEN BioResource Center. The following T-DNA insertion mutants of *CIPK3* (*cipk3*; SALK_064491C), *CIPK8* (*cipk8*; SALK_139697C), *CIPK11* (*cipk11*; SALK_108074), *CIPK26* (*cipk26*; SALK_005859C), *UBP6* (*ubp6*; SALK_206973C), and *UBP14* (*ubp14*; SALK_055277C) were obtained from Nottingham Arabidopsis Stock Centre (NASC). Homozygosity of these lines was confirmed by genomic PCR using primers recommended by the SALK database (Table 1) and they were propagated by the single seed-decent method. We could isolate homozygous lines of CIPK3, CIPK8, CIPK11 and CIPK26 as putative targets of AZD7762; UBP6 and UBP14 as putative targets of WP1130.

Growth conditions

Arabidopsis seedlings were grown hydroponically based on the method described by Kobayashi et al. (2007) in modified MGRL nutrition solution (Fujiwara et al., 1992). Briefly, the solution consisted of 2% MGRL nutrients other than $CaCl_2$ and/or phosphorous ion (Pi). The concentration of $CaCl_2$ was increased to a final concentration of 200 μM to maintain root viability. For experiments on malate secretion, Pi was removed to enhance Al toxicity, while

sucrose (1% w/v) was added to the *in vitro* culture solution to grow the seedlings. Sucrose-free medium was used for growing seedlings used in the transcription assays. The *in vitro* culture of the seedlings was conducted in a transparent plastic pot (150 mL solution), and 16 seedlings were grown separately on a 1-cm^2 mesh floated on the solution, as described by Hoekenga et al. (2003), and grown for 4 d. For transcription assays, approximately 100 seedlings were grown on a mesh supported by a photo-slide mount hydroponic culture (4 meshes per L) as described by Kobayashi et al. (2007), and the solutions were replaced every 2 d. The pH of all precultured solutions was adjusted to 5.5 and prepared in a growth room at 25 ± 1°C with a photosynthetic photon flux density of 37 μmol/m^2/s (12-h day/night cycle). All the seedlings were grown from surface-sterilized seeds that were kept in the refrigerator at 4°C for 3 d before seeding.

Root growth assay

Wild-type Col-0 were precultured in a transparent plastic pot (150 mL modified MGRL solution without Pi at pH 5.5) for 4 d as described above. For assessing effect of inhibitors on the root growth, 4-day-old seedlings were transferred the 2% MGRL nutrients (without Pi at pH 5.0) in the presence or absence (as control = 100%) of inhibitors (1 μM PIK-75, 1 μM AZD7762, 1 μM WP1130, 1 μM PAO, 25 μM LY294002, 2 μM U73122, and 2 μM U73343, respectively) for 3 h, then transferred to the 1/2 MS medium (with 1% sucrose and 1% agar at pH 5.5) for root growth. All experimental operations are carried out in a clean bench. Root elongation was measured at day 3. Five of the 10 seedlings with the longest roots are used to calculate the relative root elongation.

Quantification of malate secretion

The roots of precultured seedlings grown on mesh (16 seedlings on 1 cm^2) were transferred

into 2 mL Al-containing solution (pH 5.0, 10 μM Al of *in vitro* culture solution) in 12-well plate (1 mesh per well). The 12-well plates were continuously gently shaken using a rotary shaker (20 rpm, Multi Shaker MMS, Eyela Tokyo Rikakikai Co., Ltd., Japan) for 2 h for evaluating the effects on Al-activated malate transport by AtALMT1 or for 24 h to screen the effective chemicals, after which the malate concentrations in the solutions were quantified using the NAD/NADH cycling–coupled enzymatic method, as described previously (Kobayashi et al., 2007). 35S:*AtALMT1* seedlings were used for the experiments to evaluate the suppressing effects of the inhibitors on Al-activated malate transport by AtALMT1. Col-0 was used for screening the effective chemicals that suppress malate secretion (more detail below).

Chemical profiling of malate secretion and Al-inducible gene expression

Two hundred seventy inhibitors of signal transduction, which were used previously in human medical research (Table 2), were separately dissolved in dimethyl sulfoxide (DMSO), then, added to the solutions used for malate secretion and gene expression assays. The most effective inhibitors were identified in two screening steps as follows: 1) first screening (5 μM inhibitors) used with Col-0 to examine Al-inducible malate secretion at 24 h; 2) second screening (1 μM most effective 31 inhibitors from first screening) used with Col-0 to examine Al-inducible malate secretion at 24 h.

Three of the most effective inhibitors: PIK-75 (human PI3K inhibitor), WP1130 (human deubiquitinase inhibitor), and AZD7762 (human Chk1/Chk2 inhibitor; Table 3) were selected for further profiling of the Al-activated malate transport by AtALMT1 using the 35S:*AtALMT1* transgenic line (malate secretion for 2 h), and the expression of Al-inducible genes consisted of STOP1-regulated Al-tolerance genes *AtALMT1*, *MATE*, and *ALS3* (Sawaki et al., 2009) and Al-biomarker genes *At3g28510*, *At5g05340*, and *At5g13320* (Kobayashi et al., 2013b) in wild-type.

DNA isolation, genotyping, RNA isolation, and transcription analyses

For genotyping T-DNA insertion lines, genomic DNA was isolated using the sodium dodecyl sulfate method, and PCR-based genotyping was conducted on genomic DNA as described previously (Kobayashi et al., 2007). Total RNA was isolated from *Arabidopsis* roots using Sepasol-RNA I Super G (Nacalai Tesque) following the manufacturer's instructions. Quantitative real-time RT-PCR was conducted using SYBR premix Ex Taq II (Takara Bio) and Thermal Cycler Dice Real Time System II (Takara Bio) following the manufacturers' instructions for using gene-specific primers (Table 1). *UBQ1* (*At3g52590*) was used as an internal standard. The standard curve method of the guidelines of Bustin et al. (2009) was used to calculate all the quantifications.

Confocal microscope analysis

To investigate the effect of inhibitors on intracellular localization of STOP1, transgenic Arabidopsis (a *STOP1* promoter::STOP1-GFP reporter construct) were grown in hydroponic solution as described above (-P, pH 5.5) for 5 days. After five days growing, the seedlings were transferred to the medium (-P, pH 5.5) containing either 10 μM Al or 10 μM Al and inhibitors co-treatment for 6 h [Al treatment contained the same concentration of DMSO (0.1%)]. Florescence signal of GFP in the roots of transgenic plants were observed by using LSM-710 leaser-scanning confocal microscope (Carl Zeiss, Tokyo, Japan). GFP signal was excited at 488 nm by Argon laser and fluorescence of 493-536 nm were observed. GFP images and images merged with bright field were analyzed by software ZEISS.

Prediction of Arabidopsis proteins inhibited by human inhibitors

The targets of the inhibitors in human research were collected from the Selleck.co.jp database (http://www.selleck.co.jp). Arabidopsis targets with high homologs were predicted by using UniProtKB (https://www.uniprot.org/uniprot/) and Basic Local Alignment Search Tool (BLAST) analysis (Table 4). The PI3K/PI4K domain sequence 797–1068 (Accession number: P42336) in human p110α was used for BLAST against The Arabidopsis Information Resource (TAIR) database for detecting its Arabidopsis orthologs. *In silico* docking assay was further conducted for the most effective inhibitor, PIK-75, with Arabidopsis proteins using MODELLER (Šali and Blundell, 1993) and AutoDock Vina 1.1.2 (Trott and Olson, 2010) according to the manufacturers' instructions. The binding mode of the human PI4KIIIβ PIK-93 complex (PDB code: 4D0L) was used as the modeling template (Burke *et al.*, 2014). A grid box size of 25Å x 25Å x 25Å, centered at coordinates 8.9 (*x*), 333.3 (*y*), and 7.6 (*z*) of the PDB structure, was also used as the parameters for the docking assay. Figures were generated using UCSF Chimera (Pettersen *et al.*, 2004).

Binding of AZD7762 to its human targets viz. Chk1 and Chk2 were analyzed by docking in a similar way. This compound was found to interact with several amino acid residues in a tyrosine kinase catalytic domain within the region 1–257 (identified by Simple Modular Architecture Research Tool; Accession number: SM000220) in Chk1 and 1–267 (SM000219) in Chk2 (Letunic and Bork, 2017). These domain sequences were used for BLAST against the TAIR database for orthologous sequences in Arabidopsis. These plant orthologs were also analyzed by docking with AZD7762 (Table 5). Similarly, binding of WP1130 to its human target was also analyzed by docking (e.g. USP5). This compound was found to interact with amino acid residues in an unknown region 254–497, next to a Ubiquitin carboxyl-terminal hydrolase-like zinc finger domain (198–253; SM000290). This interacting region sequence was used for

BLAST against the TAIR database for Arabidopsis orthologs which were again analyzed for binding with WP1130 (Table 5).

3. EXPERIMENTAL RESULTS

3.1 Identification of kinase inhibitors that suppressed Al-inducible malate secretion

Effective inhibitors of Al-responsive malate secretion were identified from 270 kinase inhibitors (Table 2), which consisted of those previously used in medical science research. Most of the inhibitors were protein kinase inhibitors but also contained other kinase inhibitors, such as phosphatidyl inositol kinases. We used Al-responsive malate secretion, which comprises both transcriptional regulation (e.g., Tokizawa et al., 2015) and malate transport (e.g., Kobayashi et al., 2007), as an index for evaluating the suppressing effects of the inhibitors.

Thirty-one inhibitors suppressed malate secretion (24 h in10 μM Al, the amount of malate secretion was less than 80% compared with no-inhibitor control [100%]) at a concentration adjusted to 5 μM (Fig. 1). The 31 inhibitors comprised different types of proteins and other kinases. The inhibitors were grouped according to the target protein as follows: 1) protein tyrosine kinase/receptor (12 inhibitors), 2) serine/threonine-protein kinase/receptor (8 inhibitors), 3) phosphatidylinositol kinase (5 inhibitors), 4) mitogen-activated protein kinases (3 inhibitors), and 5) others (3 inhibitors) (Table 3). These results indicated that we could successfully identify different kinases that can regulate Al-inducible malate secretion.

The 2nd screening identified three compounds (PIK-75, AZD7762, and WP1130) as the most effective against Al-inducible malate secretion in Arabidopsis (Fig. 1C). At this step, the compounds were given at a concentration of 1 μM to reduce the possibility of cytotoxicity. At this concentration, neither expression of some of the housekeeping genes (e.g. *UBQ1*, *SAND*, and *ACT2*; Fig. 2) nor the root growth of Arabidopsis was affected by the inhibitors (Fig. 3). These three compounds interfere with different target proteins in human. The compound N-[(E)-(6-bromoimidazo[1,2-a]pyridin-3-yl)methylideneamino]-N,2-dimethyl-5-nitrobenzenesulfonamide named PIK-75 is a specific inhibitor of p110α, isoform of PI3K

(Zheng *et al.*, 2011); however, the compound 3-(carbamoylamino)-5-(3-fluorophenyl)-N-[(3S)-piperidin-3-yl]thiophene-2-carboxamide named AZD7762 is a potent selective inhibitor of cell cycle checkpoint kinases (Chk1, Chk2) that causes cell cycle arrest and allows DNA repair (Zabludoff *et al.*, 2008). Finally, the compound (E)-3-(6-bromopyridin-2-yl)-2-cyano-N-[(1S)-1-phenylbutyl]prop-2-enamide named WP1130 is identified as a partly selective deubiquitinases (DUBs) inhibitor that inhibits the activity of USP9x, USP5, USP14 and UCH37 (USP: ubiquitin-specific proteases; UCH: ubiquitin COOH-terminal hydrolase) (Kapuria *et al.*, 2010). On the other hand, putative target proteins of each compound in Arabidopsis were listed in table 5, that were highly homologous to the chemical-interacting domains in the corresponding human targets. For instance, AZD7762 was predicted inhibiting CIPKs and/or CDPKs in Arabidopsis, although its human targets are cell cycle checkpoint kinases. These three inhibitors were characterized further as to whether each inhibits a different process in Al-inducible malate secretion.

3.2 Effects of selected inhibitors on *AtALMT1* expression and malate transport by AtALMT1

Transcriptional regulation of *AtALMT1* is regulated differently in the early (e.g. 3 h) and late (>12 h) phase of Al treatment in the wild-type (Tokizawa *et al.*, 2015). Furthermore, malate transport by AtALMT1 can be immediately activated by Al, which was identified by using transgenic Arabidopsis that constitutively expresses *AtALMT1* under cauliflower mosaic virus 35S promoter (35S:*AtALMT1*). The *35S*:*AtALMT1* showed higher malate secretion than the wild-type only under Al stress but not in absence of Al (Kobayashi *et al*., 2013c). For this reason, we used the 35S:*AtALMT1* for evaluating the process of Al-activated malate transport. We profile the three selected inhibitors based on the following three regulatory factors: early and

late phases of Al-inducible expression of *AtALMT1* in wild-type (transcription at 3 and 24 h), and Al-activated malate transport using the 35S:*AtALMT1* (malate secretion after transferring to Al-containing medium from Al-free medium for 2 h; Fig. 1).

To evaluate the suppressing effect of selected inhibitors on malate transport, four-day-old transgenic plants 35S:*AtALMT1* were exposed to either 10 μM $AlCl_3$ (as control=100 %) or 10 μM $AlCl_3$ and inhibitor co-treatment medium for a short time (e.g. 2 h). Malate secretion was significantly inhibited by inhibitors PIK-75 and WP1130 (63% and 55%, respectively), while AZD7762 did not show any significantly inhibitory effect on Al-activated malate transport (Fig. 4). This result indicated that both PIK-75 and WP1130 inhibited the process of Al-activated malate transport by AtALMT1.

On the other hand, to determine effect of selected inhibitors on *AtALMT1* expression, wild-type Col-0 were incubated in the Al-containing medium in the presence or absence (control = 100%) of inhibitor for 3 h/24 h. We found that *AtALMT1* expression after 24 h in the solution containing Al was inhibited dramatically by PIK-75 (28% = inhibitor treatment to that of no-inhibitor control) and AZD7762 (28%) (Fig. 5), while the inhibitory effects were different during the early phases (3 h in Al solution). PIK-75, but not AZD7726, inhibited *AtALMT1* expression at 3 h (Fig. 5). These results indicated that PIK-75 inhibits the common and essential processes that regulate early Al-inducible *AtALMT1* expression and malate transport by AtALMT1, while AZD7726 inhibits Al-inducible *AtALMT1* expression only in the late phase of treatment and WP1130 blocks Al-activated malate transport rather than *AtALMT1* transcription.

3.3 Effect of PIK-75, AZD7762, and WP1130 on transcription of other Al-inducible genes

Expression of *AtALMT1* and other Al-tolerant genes, such as *ALS3* and *MATE*, are

coregulated by STOP1 zinc finger transcription factor (Sawaki *et al.*, 2009). However, several other genes (e.g. *At3g28510*, *At5g05340*, and *At5g13320*) are induced by 1 μM Al at pH 5.5 in the early phase of treatment, but not regulated by STOP1; thereafter, these genes can be used as Al-biomarker genes that can determine Al^{3+} contact with the surface of the PM (Kobayashi *et al.*, 2013b). The suppression effects of the inhibitors were profiled by comparing them on the expression of these genes.

PIK-75 inhibited Al-inducible expression of STOP1-regulated genes in the early phase of treatment (3 h), while other inhibitors did not affect (Fig. 6). In the late phase (24 h), PIK-75 inhibited *ALS3* expression, while AZD7762 inhibited *MATE* (Fig. 6). However, the expression of *AtSTOP1* was not affected by these inhibitors (Fig. 7). These results indicate that PIK-75 inhibits the early Al-activated process of STOP1-regulated genes without inhibiting *AtSTOP1* transcription, while AZD7762 inhibits the expression of *AtALMT1* and *MATE* in the late phase only.

The suppressing effects of the inhibitors were characterized further based on the expression of Al-biomarker genes, which are highly sensitive to Al but not regulated by STOP1 (Kobayashi *et al.*, 2013b). In this study, we also found that expression of these Al-biomarker genes was not suppressed by Al in the *stop1* mutant, compared with that in the wild-type (Fig. 8). It indicates that the transcriptional regulation of these Al-biomarker genes belongs to the STOP1-independent pathway. We observed that PIK-75, but not AZD7762, inhibited the expression of all the Al-biomarker genes in the early phase of treatment (3 h; Fig. 9). WP1130 suppressed the transcription of some of the Al-biomarker genes, even though it did not affect the expression of STOP1-regulated Al-tolerance genes (Fig. 5, 6, and 9). These results indicate that each compound, which inhibits different target proteins, differently affects Al-inducible processes.

3.4 Effects of inhibitors PIK-75 and AZD7762 on transcription of *CAMTA2* and *WRKY46*

As described, both PIK-75 and AZD7762 inhibited Al-induced *AtALMT1* expression in the late phase of treatment (24 h; Fig. 5). Our previous study has indicated that transcription factors CAMTA2 (activator of *AtALMT1*) and WRKY46 (repressor; Ding *et al.*, 2013) regulate Al-inducible *AtALMT1* expression in the late phase of treatment (Tokizawa *et al.*, 2015). We further profiled effect of PIK-75 and AZD7762 on expression of *CAMTA2* and *WRKY46* in wild-type for 24 h.

We found that AZD7762 dramatically upregulated expression of *WRKY46*, while slightly suppressed expression of *CAMTA2* (Fig. 10). This result reveals that the suppressing effect of AZD7762 on the late phase of *AtALMT1* expression primarily involves WRKY46-mediated pathway. On the other hand, PIK-75 significantly suppressed transcription levels of *CAMTA2*, as well as upregulated *WRKY46* after 24 h treatment (Fig. 10), suggesting that PIK-75 inhibited the late phases of *AtALMT1* expression involved in the transcription factors of both CAMTA2 and WRKY46.

3.5 Prediction of putative Arabidopsis proteins of the inhibitors PIK-75, AZD7762, and WP1130

According to the homology search, putative Arabidopsis proteins of PIK-75, AZD7762, WP1130 were predicted as PI3K/PI4Ks, CIPKs/CDPKs, and UBPs, respectively, with similar docking scores (Table 5). Furthermore, *in silico* binding assay with the most effective inhibitor PIK-75 also found that the orthologs PI3K/PI4Ks in Arabidopsis can bind with PIK-75 at the interacting domains (Fig. 11). Similarly, the Arabidopsis proteins CIPK3, CIPK8, CIPK11, CIPK26 and so on, were predicted as candidates of AZD7762; UBP6, UBP14 and so on, were predicted as candidates of WP1130; PI3K, PI4Kβ2, PI4Kβ1, PI4Kα2, and PI4Kα1 were

predicted as candidates of PIK-75 (Table 5).

3.6 Characterization of Al-inducible malate secretion and *AtALMT1* expression in the roots of *UBP* and *CIPK* T-DNA insertion mutants

To validate the role of UBP and CIPK in the regulation of Al-inducible malate secretion as suggested by our pharmacological assays, we analyzed *AtALMT1* expression and malate release in the available T-DNA insertion mutants of *CIPKs* and *UBPs*, respectively. Since WP1130 suppressed malate secretion in 35S:*AtALMT1* rather than Al-inducible *AtALMT1* expression in wild-type (Fig. 4 and 5), we analyzed the malate secretion in the T-DNA insertion mutants of *UBP*. However, we could not find a significant reduction of malate secretion in these mutants, which may be attributed to genetic redundancy (Fig. 12; Liu et al., 2008). On the other hand, even though AZD7762 significantly inhibited the late-phase Al-inducible *AtALMT1* expression, we failed to detect significant suppression of *AtALMT1* expression in the single T-DNA insertion mutants of some of the putative targets of AZD762 such as *CIPK3*, *CIPK8*, *CIPK11* and *CIPK26*, which may be due to genetic redundancy (Fig. 12).

4. DISCUSSION

Al-inducible malate secretion in Arabidopsis is controlled by both *AtALMT1* expression and malate transport by AtALMT1 (Hoekenga *et al.*, 2006; Kobayashi *et al.*, 2007; Ligaba *et al.*, 2009). We identified the different regulatory mechanisms of each process using a pharmacological approach with a library of various types of compounds, which affect different signaling pathways in human cells (Table 3). In addition, we employed lower concentrations of these chemicals at the 2nd screening, by which we could minimize their cytotoxic effects. Under these concentrations, expression of some of the housekeeping genes and the root growth were not affected by the inhibitors (Fig. 2 and 3). But we might exclude effective compounds that block Al-inducible malate secretion if their uptake or biological activity reduced at low concentration. Despite such limitations, we succeeded to identify three inhibitors (PIK-75, AZD7762, and WP1130) that suppressed Al-inducible malate secretion differently as follows: 1) AZD7762 affected Al-induced *AtALMT1* expression in the late phase of treatment, 2) WP1130 inactivated malate transport activity, and 3) PIK-75 inhibited both malate transport activity and *AtALMT1* expression (Fig. 4 and 5).

AZD7762 is identified as a potent selective inhibitor of cell cycle checkpoint kinases (Chk1 and Chk2; Table 3), which belongs to the damaged DNA repairing pathway (DDR pathway). However, putative target proteins of AZD7762 are CIPKs and CDPKs in Arabidopsis as predicted by a homology search against the interacting domain of the Chk1/Chk2 in humans (Table 4), even though inhibition of the DDR pathway maintains root growth (e.g. inhibits the active process for stopping root growth by sensing DNA damage in Al treatment) (Eekhout *et al.*, 2017). CBL1 is already known to be involved in upregulating *AtALMT1* (Ligaba-Osena *et al.*, 2017). Additionally, CDPKs might also regulate *AtALMT1* expression, because AZD7762 bind *in silico* to both CIPKs and CDPKs with similar affinity (Table 4) and CDPKs reportedly

enhance a group of specific WRKY transcription factors (Gao *et al.*, 2013, 2014). Our results strongly suggest that AZD7762 inhibited the late phase of *AtALMT1* expression primarily through the WRKY46-mediated pathway, but may also include CAMTA2, because AZD7762 significantly upregulated expression of *WRKY46* while *CAMTA2* was slightly suppressed (Fig. 10). However, we failed to detect significant suppression of *AtALMT1* expression in the single T-DNA insertion mutants of some of the putative targets of AZD762 such as *CIPK3*, *CIPK8*, *CIPK11* and *CIPK26*, which may be due to genetic redundancy (Fig. 12).

On the other hand, we found that WP1130 suppressed malate secretion in 35S:*AtALMT1* rather than Al-inducible *AtALMT1* expression in wild-type (Fig. 4 and 5). This indicates that WP1130 blocks the process of Al-activated malate transport by AtALMT1 rather than expression of *AtALMT1*. In fact, the small-molecule WP1130 can inhibit deubiquitinases such as ubiquitin-specific proteases (UBPs), as predicted by a homology search against the interacting domain of the USPs in humans (Table 4). In plants, UBPs reportedly participate in signal transduction under Pi-starvation (Li *et al.*, 2010) and biotic stress (Ewan *et al.*, 2011). These stimuli are also known to activate ALMT1-dependent malate secretion (Rudrappa *et al.*, 2008; Kobayashi *et al.*, 2013a; Balzergue *et al.*, 2017). However, we could not find a significant reduction of malate secretion in the T-DNA insertion mutants of *UBP* which may be attributed to genetic redundancy (Fig. 12; Liu *et al.*, 2008). Although the molecular mechanisms of deubiquitinases regulating malate transport are still unclear, our findings suggest a possible role of UBPs in Al-activated malate transport by AtALMT1.

Clear inhibitory effects of PIK-75 occurred during the early phase of Al treatment, which inhibited both Al-inducible expression of *AtALMT1* and Al-activated malate transport by AtALMT1 (Fig. 4 and 5). Furthermore, homology search and *in silico* binding assay identified that it can inhibit both PI3K and PI4Ks in Arabidopsis (Table 4, Fig. 11). These findings suggest

that phosphatidylinositol (PtdIns) metabolism could play important roles in the early Al-inducible malate secretion, including activation of both *AtALMT1* expression and malate transporter activity. However, there is a dearth of information about PtdIns-signals in plants under Al stress. Jones and Kochian (1995; 1997) previously reported that PtdIns metabolism pathway may involve in early Al signaling; however, its relationship to Al-inducible malate secretion has not been clarified. Further characterization of the PtdIns inhibitors on would be useful for profiling of PtdIns metabolisms interfere with Al-inducible malate secretion.

Overall, these inhibitors exhibited differently inhibitory effect on the complex regulation of Al-responsive AtALMT1 signaling pathway in *Arabidopsis thaliana*. Firstly, targets of inhibitor PIK-75 belong to the up-stream of Al-responsive AtALMT1 signaling pathway: releasing multiple signals to down-stream responses, including early activation of malate transport activity and Al-inducible *AtALMT1* expression. Secondly, inhibitor AZD7762 blocked Al-induced *AtALMT1* expression in the late phase through activating *WRKY46* expression. Finally, inhibitor WP1130 decreased malate release mainly dependents on inactivation of malate transporter ALMT1. As WP1130 displayed inhibitory effect on expression of some of Al-biomarkers, suggests that its targets also involve in the other early Al-responsive signals transduction pathway. Besides, we also found that PIK-75, but not AZD7762, inhibited the early activated process of STOP1-regulated genes (e.g. *AtALMT1*, *ALS3*, and *MATE*) without inhibiting *STOP1* transcription. This suggests that PIK-75 block the process of STOP1 accumulation to nucleus, that was further confirmed by the confocal microscope analysis that PIK-75 greatly blocked intracellular localization of STOP1 into nucleus, while AZD7762 exhibited similar GFP signals with Al treatment (Fig. 13). Taken all, our findings herein firstly discovered that there may be a common mechanism in Al-induced *AtALMT1* expression and AtALMT1 transport protein activity.

Table 1. Sequence information of PCR primers for quantitative RT-PCR, genomic PCR, and cloning

PCR category		Sequence (5' to 3')	
		Forward primer sequence	Reverse primer sequence
Real-time RT-PCR	*AtALMT1*(At1g08430)	TCTTCATGTTTTTCATGGTTTGAGTT	CACAGTTTTACATGACGTTGATAATGAT
	ALS3 (At2g37330)	TATCGATCCTTGCCGGGACTTCA	GCTTGTCTTGGCGTTGCTCCTA
	AtMATE (At1g51340)	CCTTAGCGTTTGTGTTCGATGGAG	ACCATGAGTCGATGAGAGGAAGAG
	At3g28510	AATACGTCCCTGCCCATTTC	TCGTAGGCTTGGCTTCTCTTC
	At5g13320	TGCCCTAACAACACCGAAAG	GAACCCGTCCTCACAACCTC
	At5g05340	CTCTTCAACGGCGGCTCTAC	CAAACCTTGCGGATTTCACC
	CAMTA2 (At5g64220)	CACCCAGTGGTTCACTCTTTCTC	TGCCCGTCTTTTCGGAAATA
	WRKY46 (At2g46400)	ACATCACATCCCCGAAGACG	ACTTCTTCGGACTTGGTCGG
	AtSTOP1 (At1g34370)	TTTCCGCGACTGATGTTTGAT	ACAGGCATTCGCAATAAGCAT
	NtMATE	CAGCATTGTGTTCTTGCTCATTC	TGGTTTCGGGAGGATAGGC
	NtActin	AACCCCAAGGCCAATAGAGAA	GAGACACCATCACCAGAATCCA
Genomic PCR	*UBQ1* (At3g52590)	TCGTAAGTACAATCAGGATAAGATG	CACTGAAACAAGAAAAACAAACCCT
	PI4Kα1 (At1g49340)	CGATTCGAGAGTGCTCATTTC	AACAATATTGCGATGGACAGC
	PI4Kα2 (At1g51040)	ATCACCAGGGTGAGTCTGTTG	TCAATAATACCCTTCCCGGAC
	PI4Kβ1 (At5g64070)	AGGACGTAACCAGAGGGGTAG	CGTTGTGACCCGTCATTAATC
	PI4Kβ2 (At5g09350)	ATGAACGAAATTGGGTTCTCC	AAACCTCCTTATCTTCCGCTG
	CIPK3 (At2g26980)	TACTGGTTGTTGTTGTTGCAGG	TAGTGATGAGTTTCATGGCACC
	CIPK8 (At4g24400)	TCGTGGATCGTAGCACA	ACCCCACAGGACCAAA
	CIPK11 (At2g30360)	CAATCCCGACGAGTAAGAAATC	TATCTTTTTAAAAGCTTCCGCG
	CIPK26 (At5g21326)	AGCATAAGATGGCTGAACAGG	CAGGAGCAGCATAGTTTGGAG
	UBP6 (At1g51710)	AGGAGGAGTTTACGGCAGAAG	CTTGGCAACACGTGTTACATG
	UBP14 (At3g20630)	GAGTATTGTTATCCCGCGATTC	GCTTTACCGGAGTATCGAAGG

Cloning	*PI3K* (At1g60490)	AAAAAGCAGGCTGATTTCACTCTTCCTCAAATGAAAAAGCC	AGAAAGCTGGGTAGCAGTATGGTGGTCCTGTAG

Table 2. List of inhibitors used for characterizing signal transduction pathway of Al-inducible malate secretion of *Arabidopsis thaliana*.

	1	2	3	4	5	6	7	8	9	10	11	12
a	Dovitinib (TKI-258)	BMS-599626 (AC480)	Erlotinib HCl	Gefitinib (Iressa)	Neratinib (HKI-272)	PD153035 HCl	Pelitinib (EKB-569)	Vandetanib (Zactima)	WZ3146	WZ4002	WZ8040	IMD 0354
b	Tivozanib (AV-951)	Axitinib	BIBF1120 (Vargatef)	BMS 794833	Piceatannol	Cediranib (AZD2171)	Y-27632 2HCl	CYC116	PHA-665752	Imatinib (Gleevec)	Imatinib Mesylate	WHI-P154
c	Ki8751	KRN 633	Masitinib (AB1010)	MGCD-265	Motesanib Diphosphate	Amuvatinib (MP-470)	OSI-930	Pazopanib HCl	Sorafenib (Nexavar)	Sunitinib Malate (Sutent)	TSU-68	TG 100713
d	Vatalanib dihydrochloride (PTK787)	Foretinib (GSK1363089, XL880)	Danusertib (PHA-739358)	AT9283	Saracatinib (AZD0530)	Bosutinib (SKI-606)	Dasatinib (BMS-354825)	Nilotinib (AMN-107)	Quercetin (Sophoretin)	NVP-ADW742	Quizartinib (AC220)	Torin 2
e	Ponatinib (AP24534)	Tandutinib (MLN518)	KW 2449	CI-1033 (Canertinib)	CP-724714	Regorafenib (BAY 73-4506)	JNJ-38877605	PF-04217903	Crizotinib (PF-02341066)	Brivanib (BMS-540215)	SGX-523	NVP-TAE226
f	SU11274	TAE684 (NVP-TAE684)	SB 525334	R406	R406 (free base)	XL-184 free base (Cabozantinib)	BI 2536	GSK461364	HMN-214	Rigosertib (ON-01910)	AT7519	Tideglusib

g	Linsitinib (OSI-906)	BS-181 HCl	PD 0332991 (Palbociclib) HCl	PHA-793887	Roscovitine (Seliciclib, CYC202)	SNS-032 (BMS-387032)	AZD7762	Aurora A Inhibitor I	Barasertib (AZD1152-HQPA)	CCT129202	ENMD-2076	TPCA-1
h	Hesperadin	MLN8237 (Alisertib)	GSK1904529A	PHA-680632	SNS-314	VX-680 (MK-0457, Tozasertib)	ZM-447439	AS703026	AZD6244 (Selumetinib)	AZD8330	BIX 02188	Desmethyl Erlotinib (CP-473420)
i	BIX 02189	BMS 777607	CI-1040 (PD184352)	PD318088	PD0325901	PD98059	U0126-EtOH	LY2228820	BIRB 796 (Doramapimod)	SB 202190	SB 203580	Torin 1
j	MLN8054	VX-702	Dovitinib Dilactic acid (TKI258 Dilactic acid)	GDC-0879	OSU-03012	PLX-4720	Dinaciclib (SCH727965)	SP600125	GSK690693	AS-605240	GDC-0941	SAR131675
k	IC-87114	LY294002	PIK-293	PIK-90	PIK-93	TG100-115	TGX-221	XL147	XL765	ZSTK474	AZD8055	Semaxanib (SU5416)
l	Deforolimus (Ridaforolimus)	Everolimus (RAD001)	KU-0063794	Rapamycin (Sirolimus)	Temsirolimus (Torisel)	WYE-354	Triciribine (Triciribine phosphate)	PIK-75 Hydrochloride	Brivanib alaninate (BMS-582664)	Indirubin	SB 216763	Baricitinib (LY3009104)

m	KU-55933	KU-60019	MK-2206 dihydrochloride	E7080 (Lenvatinib)	AT7867	YM201636	INK 128	AG-1024	LY2784544	PD173074	Enzastaurin (LY317615)	Golvatinib (E7050)
n	Vemurafenib (PLX4032)	BX-795	SB 431542	Linifanib (ABT-869)	AEE788 (NVP-AEE788)	Afatinib (BIBW2992)	Lapatinib Ditosylate (Tykerb)	JNJ-7706621	BX-912	BEZ235 (NVP-BEZ235)	GSK1059615	Tyrphostin AG 879 (AG 879)
o	PI-103	AG-490	Tofacitinib citrate (CP-690550 citrate)	Crenolanib (CP-868596)	GSK1838705A	KX2-391	NVP-BSK805	PCI-32765 (Ibrutinib)	PF-00562271	DCC-2036 (Rebastinib)	LDN193189	BYL719
p	AZD8931	Raf265 derivative	NVP-BHG712	OSI-420 (Desmethyl Erlotinib)	R935788 (Fostamatinib disodium)	AZ 960	Mubritinib (TAK 165)	PP242	Cyt387	Apatinib (YN968D1)	CAL-101 (GS-1101)	GDC-0068
q	PIK-294	AMG-208	Telatinib (BAY 57-9352)	BI6727 (Volasertib)	WP1130	BKM120 (NVP-BKM120)	cx-4945 (Silmitasertib)	Phenformin hydrochloride	TAK-733	AZD5438	PP-121	Dabrafenib (GSK2118436)
r	OSI-027	LY2603618 (IC-83)	PF-05212384 (PKI-587)	CCT128930	A66	NU7441 (KU-57788)	GSK2126458	WYE-125132	WYE-687	A-674563	AS-252424	CEP33779
s	GSK1120212 (Trametinib)	Flavopiridol hydrochloride	AS-604850	WAY-600	TG101209	GDC-0980 (RG7422)	A-769662	TAK-901	AMG 900	ZM 336372	Ruxolitinib (INCB018424)	AZD4547

t	PH-797804	PF-04691502	Staurosporine	Thiazovivin	WP1066	CP 673451	PHT-427	Tie2 kinase inhibitor	Sotrastaurin (AEB071)	BMS-265246	BGJ398 (NVP-BGJ398)	Tofacitinib (CP-690550, Tasocitinib)
u	AST-1306	SB590885	Palomid 529	R788 (Fostamatinib)	CAY10505	CHIR-124	PF-03814735	Dacomitinib (PF299804,PF-00299804)	AG-1478 (Tyrphostin AG-1478)	SB 415286	INCB28060	TAK-285
v	TG101348 (SAR302503)	PKI-402	GSK1070916	PHA-767491	CCT137690	CHIR-98014	AZD2014	AMG458	NVP-BGT226	PHA-848125	Arry-380	MK-2461
w	MK-5108 (VX-689)	ARRY334543	Wortmannin	NVP-BVU972	CH5424802	3-Methyladenine						

Table 3. Target proteins of 31 inhibitors in *Homo sapiens* (*human*), which were most effective to inhibit malate secretion from the roots of Arabidopsis in Al medium.

Inhibitor	Target in human	Description
PIK-75 Hydrochloride	p110α	PI3K
BMS 794833	VEGFR	protein tyrosine kinase (receptor)
GDC-0879	B-Raf	serine/threonine-specific protein kinase
AZD7762	Chk1, Chk2	serine/threonine-specific protein kinase
Linifanib (ABT-869)	VEGFR/PDGFR	protein tyrosine kinase (receptor)
TAK-285	HER2 and EGFR(HER1)	protein tyrosine kinase (receptor)
CI-1033 (Canertinib)	EGFR and ErbB2 (HER2)	protein tyrosine kinase (receptor)
PIK-90	PI3Kα/γ/δ	PI3K
Neratinib (HKI-272)	HER2 and EGFR	protein tyrosine kinase (receptor)
WP1130	USP9x, USP5, USP14 and UCH37	deubiquitinase
SB 431542	ALK5	serine/threonine kinase (receptor)
E7080 (Lenvatinib)	VEGFR2(KDR)/VEGFR3(Flt-4)	protein tyrosine kinase (receptor)
GSK1904529A	IGF-1R/IR	protein tyrosine kinase (receptor)
BX-795	PDK1	phosphoinositide-dependent kinase-1
KU-60019	ATM	serine/threonine kinase
CP-724714	HER2/ErbB2	protein tyrosine kinase (receptor)
PHA-680632	Aurora Kinase A/B/C	serine/threonine-protein kinases
PIK-293	PI3Kδ	PI3K
AT7867	Akt1/2/3 and p70S6K/PKA	serine/threonine kinase
TAK-901	Aurora Kinase A/B	serine/threonine-protein kinases
CI-1040 (PD184352)	MEK1/2	mitogen-activated protein kinase kinase
Phenformin hydrochloride	AMPK (activator)	5' adenosine monophosphate-activated protein kinase

PD318088	MEK1/2	mitogen-activated protein kinase kinase
GSK690693	Akt1/2/3	serine/threonine kinase
Cyt387	JAK1/JAK2	protein tyrosine kinase
AEE788 (NVP-AEE788)	EGFR and HER2/ErbB2	protein tyrosine kinase (receptor)
R406	Syk	tyrosine-protein kinase
3-Methyladenine	Vps34 and PI3Kγ	PI3K
PIK-93	PI3Kα	PI3K
Mubritinib (TAK 165)	HER2/ErbB2	protein tyrosine kinase (receptor)
PD0325901	MEK	mitogen-activated protein kinase kinase

*Pre-grown Arabidopsis roots were exposed to Al containing medium (10 μM Al at pH 5.0) for 24 hours in the presence of inhibitors (5 μM). The inhibitors showed most effectively inhibited malate secretion are listed with the target proteins in human as well as their descriptions.

Table 4. Arabidopsis proteins that have high homology to human target proteins of PIK-75, WP1130, and AZD7762.

Inhibitor	AGI code	Gene Name	E value in homology search	% Identity	Docking Score (kcal/mol)
PIK-75	AT1G49340	phosphatidylinositol 4-kinase *alpha*1	4.00E-36	34%	-8.5
	AT1G60490	phosphatidylinositol 3-kinase	4.13E-36	34%	-8.3
	AT1G51040	phosphatidylinositol 4-kinase *alpha 2*	1.40E-31	34%	-8.6
	AT5G09350	phosphatidylinositol 4-kinase *beta*2	7.81E-28	32%	-9.7
	AT5G64070	phosphatidylinositol 4-kinase *beta* 1	1.52E-27	31%	-9.1
WP1130	AT3G20630	ubiquitin-specific protease 14	8.00E-63	43%	-5.5
	AT2G22310	ubiquitin-specific protease 4	1.00E-07	24%	-7.8
	AT2G40930	ubiquitin-specific protease 5	3.00E-07	35%	-5.3
	AT1G51710	ubiquitin-specific protease 6	8.00E-07	32%	-6.9
	AT4G39910	ubiquitin-specific protease 3	1.00E-06	25%	-7.4
AZD7762	AT5G21326	CBL-interacting protein kinase 26	5.00E-51	40%	-8.1
	AT4G24400	CBL-interacting protein kinase 8	5.00E-50	41%	-8.7
	AT2G26980	CBL-interacting protein kinase 3	1.00E-49	40%	-8.7
	AT2G30360	CBL-interacting protein kinase 11	5.00E-47	39%	-8.7
	AT5G21222	protein kinase family protein	1.00E-46	39%	-8.1
	AT4G04720	calcium-dependent protein kinase 21	1.00E-40	39%	-8.4
	AT1G50700	calcium-dependent protein kinase 33	2.00E-40	39%	-8.1

*AGI code, gene name, E value and % Identity were obtained from BLASTP using functional domains of human target proteins (PIK-75, PI3K/PI4K domain 797-1068 (Accession number: P42336) in human p110α; WP1130, unknown domain 254-497 in human USP5 which next to the Znf UBP domain 198-253 (Accession number: SM000290); AZD7762, tyrosine kinase catalytic domain 1-257 (SM000220) in human Chk1 and 1-267 (SM000219) in human Chk2).

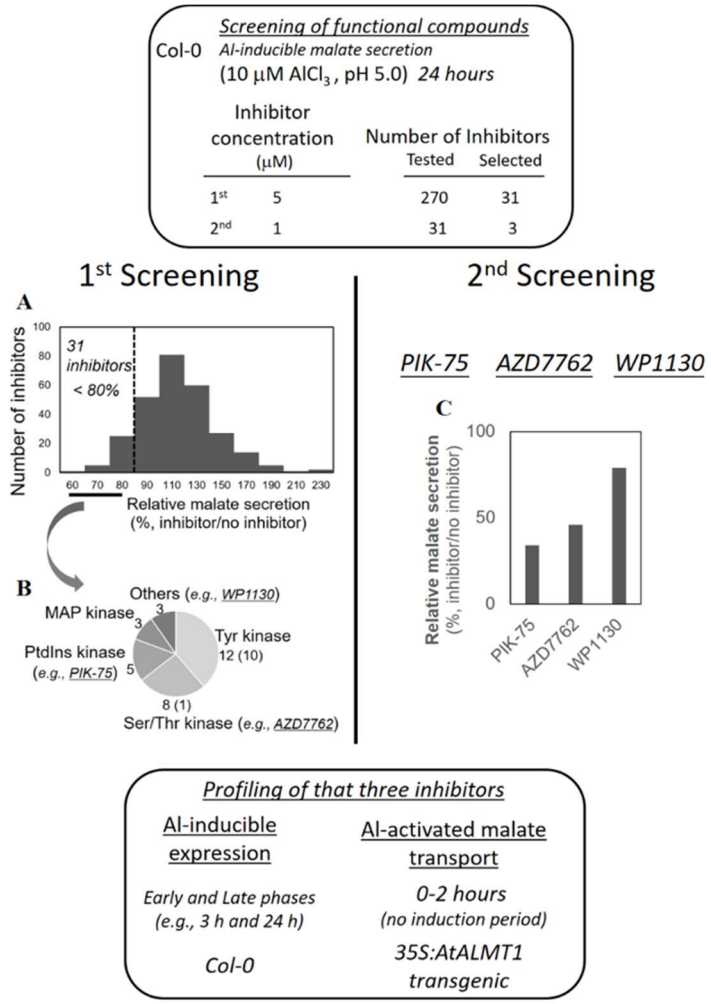

Figure 1. Schematic representation of chemical screening of effective inhibitors in Al-inducible malate secretion in Arabidopsis. Roots of the 4-day-old seedlings of wild-type Col-0 were exposed to Al-containing solution (10 μM $AlCl_3$ at pH 5.0) in the presence or absence (as control = 100%) of inhibitors for 24 h. (**A**) Distribution of malate secretion in the roots of wild-type under cotreatment with Al and inhibitors (5 μM). (**B**) Thirty-one inhibitors that suppressed malate secretion more than 20% were selected from the first screening shown in the panel A. The 31 inhibitors comprised different types of protein- and other-kinases, and other signal transducers. (**C**) Malate secretion in the roots of wild-type under cotreatment with Al and most effective inhibitors (1 μM) that were consisted of PIK-75, AZD7762, and WP1130. Relative malate secretion (%, inhibitor/no inhibitor) compared with that of no-inhibitor control is shown. These inhibitors were characterized further as to whether each inhibits a different process in Al-responsive malate secretion.

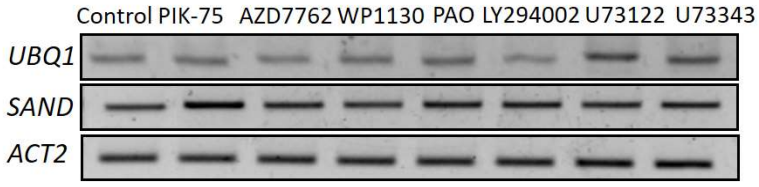

Figure 2. RT-PCR analysis of *UBQ1* (*At3g52590*), *SAND* (*At2g28390*), and *ACT2* (*At3g18780*) transcripts in wild-type under stress conditions. Roots of the 10-day-old seedlings of wild-type Col-0 were exposed to Al containing solutions (10 μM $AlCl_3$ at pH 5.0) in the presence or absence (as control) of inhibitors (1 μM PIK-75, 1 μM AZD7762, 1 μM WP1130, 1 μM PAO, 25 μM LY294002, 2 μM U73122, and 2 μM U73343, respectively) for 3 h. RT-PCR analysis uses the primers specific for *UBQ1* (Forward: TCGTAAGTACAATCAGGATAAGATG; Reverse: CACTGAAACAAGAAAAACAAACCCT), *SAND* (Forward: GGGACCCCACAAGACTCAATA; Reverse: CATCTTTTACCCTTTGGCACAC) and *ACT2* (Forward: GGCAAGTCATCACGATTGG; Reverse: CAGCTTCCATTCCCACAAAC).

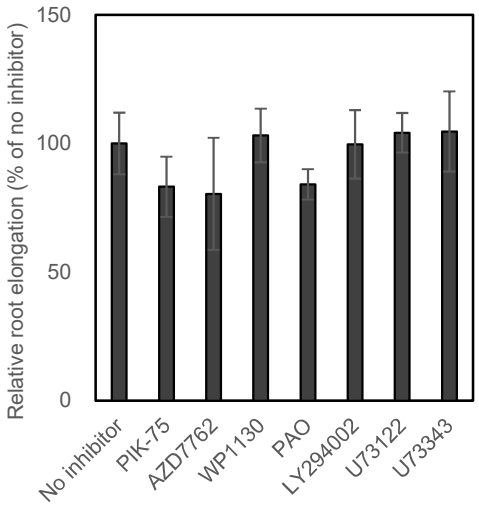

Figure 3. Effects of the inhibitors on the root growth of wild-type Arabidopsis. Seedlings were precultured in a transparent plastic pot (150 mL modified MGRL solution without Pi at pH 5.5) for 4 d as described in the materials and methods. For assessing effect of inhibitors on the root growth, 4-day-old seedlings were transferred the 2% MGRL nutrients (without Pi at pH 5.0) in the presence or absence (as control = 100%) of inhibitors (1 μM PIK-75, 1 μM AZD7762, 1 μM WP1130, 1 μM PAO, 25 μM LY294002, 2 μM U73122, and 2 μM U73343, respectively) for 3 h, then transferred to the 1/2 MS medium (with 1% sucrose and 1% agar at pH 5.5) for root growth. All experimental operations are carried out in a clean bench. Root elongation was measured at day 3. Five of the 10 seedlings with the longest roots are used to calculate the relative root elongation. Values are means ± SD (n = 5).

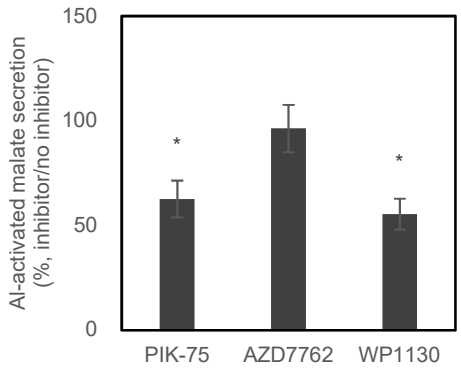

Figure 4. Al-activated malate secretion in the roots of transgenic plants 35S:*AtALMT1*. Four-day-old seedlings (*in vitro* culture) of 35S:*AtALMT1* were transferred to Al-containing solutions (10 μM $AlCl_3$ at pH 5.0) in the presence or absence (as control = 100%) of 1 μM inhibitors for 2 h. The means of relative malate secretion (%, inhibitor/no inhibitor) ± SD values of the three replicates are shown. Asterisks in each treatment represent significant differences compared with control conditions (no inhibitor = 100%) (LSD test; *, $P < 0.05$).

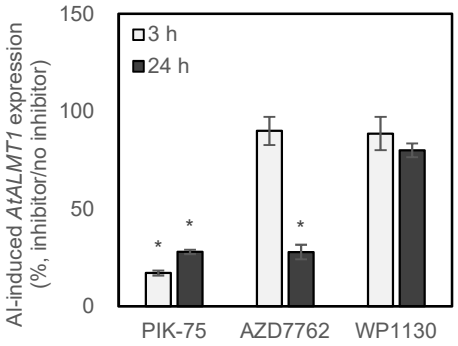

Figure 5. Al-inducible *AtALMT1* expression in the roots of wild-type. Roots of the 10-day-old seedlings of wild-type were exposed to Al-containing solutions (10 μM $AlCl_3$ at pH 5.0) in the presence or absence (as control = 100%) of 1 μM inhibitors. *AtALMT1* expression at 3 and 24 h were quantified by quantitative real-time reverse transcription-polymerase chain reaction (RT-PCR) using *UBQ1* as an internal control. The means of relative expression levels (%, inhibitor/no inhibitor) ± SD values with three replicates are shown. Asterisks in each treatment represent significant differences compared with control conditions (no inhibitor = 100%) (LSD test; *, $P < 0.05$).

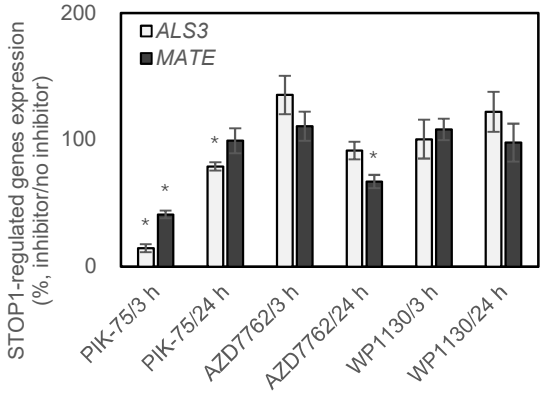

Figure 6. Effect of inhibitors (PIK-75, AZD7762 and WP1130) on the expression of STOP1-regulated genes in the roots of wild-type. The roots of 10-day-old precultured seedlings in the Al-free solution were exposed to Al (10 μM $AlCl_3$ at pH 5.0) in the presence or absence of inhibitors (1 μM). Conditions of treatment were identical to those described in Fig. 5. Effects on the expression of STOP1-regulated genes, seedlings were incubated in Al-containing solutions for 3 h and 24 h, respectively. The means of relative Al-inducible expression (%, inhibitor/no inhibitor) ± SD values of the three replicates are shown. Asterisks in each treatment represent significant differences from those under control conditions (no inhibitor = 100%) (LSD test; *, $P < 0.05$).

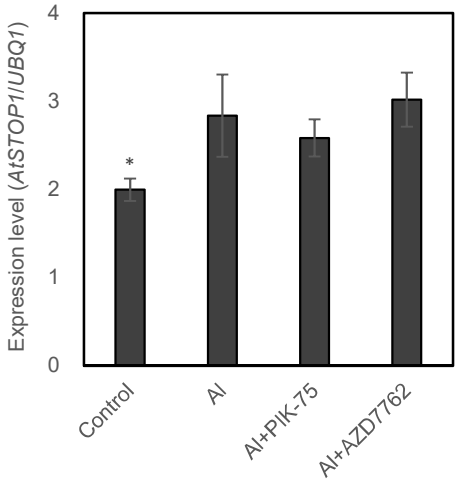

Figure 7. Effect of inhibitors on expression of *AtSTOP1* in wild-type. The roots of 10-day-old precultured seedlings in the Al-free solutions were exposed to Al containing medium (10 μM $AlCl_3$ at pH 5.0) in the presence or absence of inhibitors for 3 h, using -Al as a control. Expression level of *AtSTOP1* was quantified by quantitative real-time RT-PCR using *UBQ1* as an internal control. The means of expression level (*AtSTOP1*/*UBQ1*) ± SD values with three replicates are shown. Asterisks in each treatment represent significant differences compared with Al treatment (LSD test; *, $P < 0.05$).

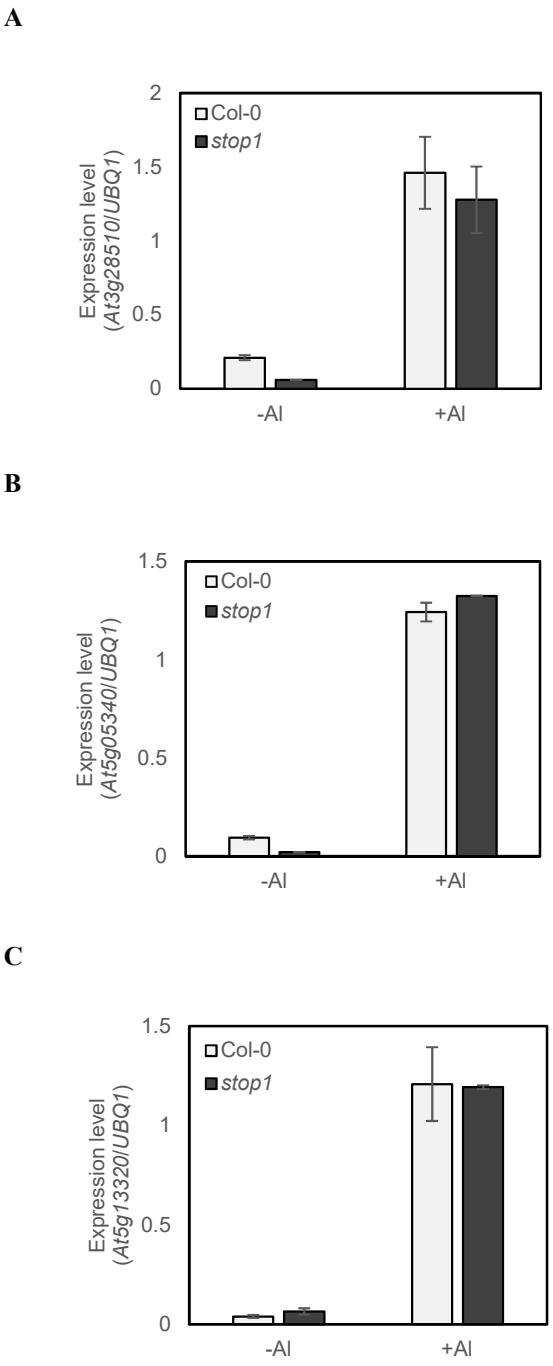

Figure 8. Expression of Al-biomarker genes in the roots of wild-type and *stop1* mutant. The roots of 10-day-old precultured seedlings in the Al-free solutions were exposed to Al containing medium (10 μM $AlCl_3$ at pH 5.0) for 3 h. Al-inducible expression of Al-biomarker genes were quantified by quantitative real-time RT-PCR using *UBQ1* as an internal control. The means of expression levels (genes/*UBQ1*) ± SD values with three replicates are shown. Asterisks in each treatment represent significant differences compared with wild-type Col-0 (LSD test; *, $P < 0.05$).

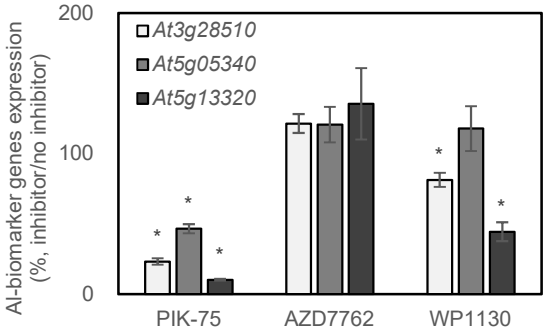

Figure 9. Effect of inhibitors (PIK-75, AZD7762 and WP1130) on the expression of Al-biomarker genes in the roots of wild-type. The roots of 10-day-old precultured seedlings in the Al-free solution were exposed to Al (10 μM $AlCl_3$ at pH 5.0) in the presence or absence of inhibitors (1 μM). Conditions of treatment were identical to those described in Fig. 5. Effects on the expression of Al-biomarker genes, seedlings were incubated in inhibitors-containing solution for 3 h. The means of relative Al-inducible expression (%, inhibitor/no inhibitor) ± SD values of the three replicates are shown. Asterisks in each treatment represent significant differences from those under control conditions (no inhibitor = 100%) (LSD test; *, $P < 0.05$).

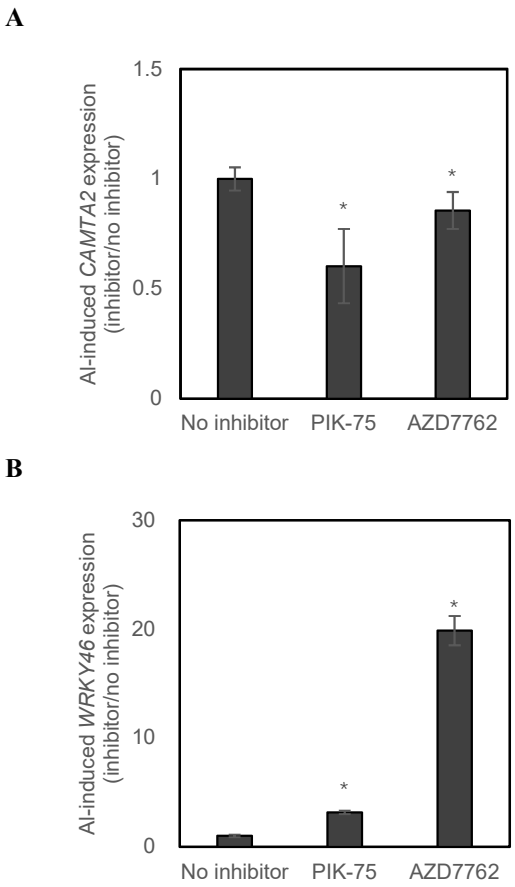

Figure 10. Effects of inhibitors PIK-75 and AZD7762 on expression of *CAMTA2* and *WRKY46* in wild-type. Roots of the 10-day-old seedlings of wild-type Col-0 were exposed to Al containing solutions (10 μM $AlCl_3$ at pH 5.0) in the presence or absence (as control = 1) of 1 μM inhibitor for 24 h. The effects of inhibitor on expression levels of *CAMTA2* (*AtALMT1* activator) (**A**) and *WRKY46* (*AtALMT1* repressor) (**B**) in wild-type were quantified by quantitative real-time RT-PCR using *UBQ1* as an internal control. The asterisks in each treatment represent significant differences compared with no-inhibitor (as control = 1) (LSD test; *, $P < 0.05$). The mean ± SD values of the three replicates are shown.

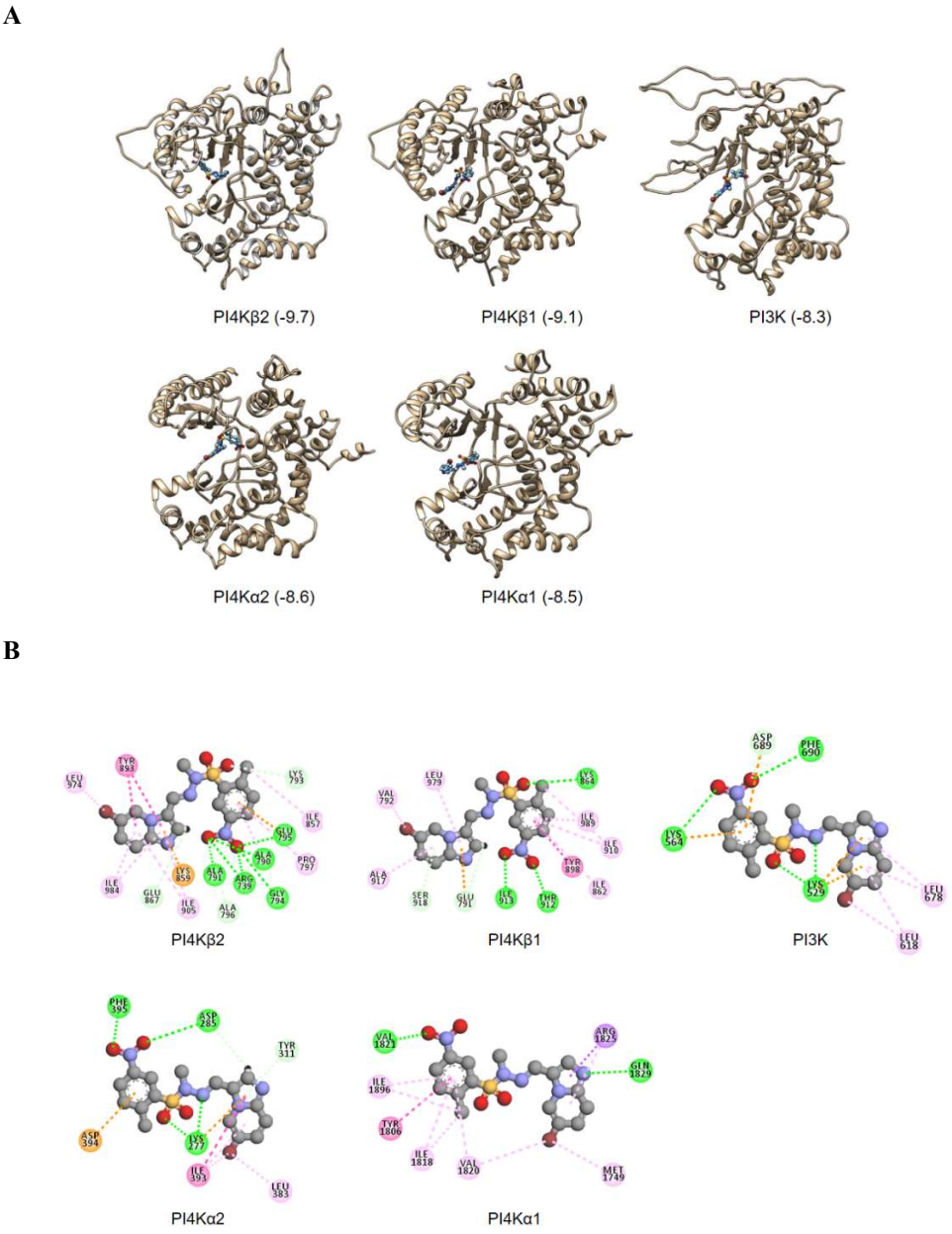

Figure 11. Characterization of PIK-75 interacts with Arabidopsis PI3K and PI4Ks by *in silico* docking assay. To obtain information of the structural basis of the observed activity of PIK-75 against Arabidopsis proteins, we performed molecular docking using a validated molecular dock program. Structural models of the individual PIKs were built with MODELLER (Šali and Blundell, 1993) based on the sequence alignment between PIKs and the template structure human PI4KIIIβ PIK-93 complex (PDB code: 4D0L) (Burke *et al.*, 2014). PIK-75 was docked with the functional domain of each protein using each modeled structure and AutoDock Vina 1.1.2 (Trott and Olson, 2010). (**A**) Top-scored binding modes of PIK-75 with the functional domain of each protein. Docking scores of PIK-75 with each homologous protein were shown in the brackets (kcal/mol). (**B**) Interactions of each homologous protein with PIK-

75. The possible amino acids residues (e.g. ALA represents Alanine, ARG represents Arginine and so on) that interact with PIK-75 are shown. PIK-75 is shown in ball-and-stick representation. Green dotted lines represent putative hydrogen bonds. Other dotted lines represent putative hydrophobic interactions, such as π-π, π-alkyl (magenta) and π-cation or anion interactions (orange). The figures were generated using UCSF Chimera (Pettersen *et al.*, 2004).

A

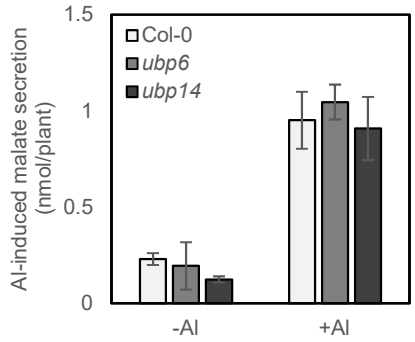

B

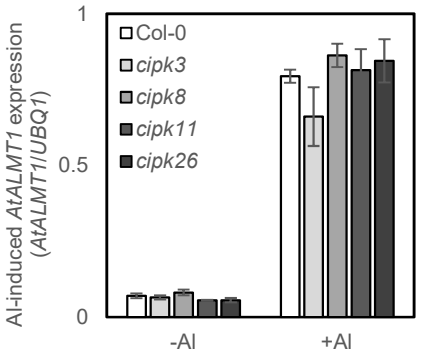

Figure 12. Malate secretion in the roots of T-DNA insertion mutants of *UBP* and Al-induced *AtALMT1* expression in the roots of T-DNA insertion mutants of *CIPK* under Al exposure. (**A**) malate secretion in the roots of T-DNA insertion mutants of *UBP*. Four-day-old seedlings (*in vitro* culture) of *UBP* mutants and wild-type Col-0 were transferred to Al-containing solution (10 μM $AlCl_3$ at pH 5.0) for 24 h. (**B**) *AtALMT1* expression levels in the roots of *CIPK* mutants and wild-type Col-0. Roots of the 10-day-old seedlings of *CIPK* mutants were exposed to modified MGRL medium in the presence or absence (as control) of 10 μM $AlCl_3$ at pH 5 for 24 h. *AtALMT1* expression levels were quantified by quantitative real-time RT-PCR using *UBQ1* as an internal control. The means ± SD values with three replicates are shown. Asterisks in each treatment represent significant differences compared with wild-type Col-0 (LSD test; *, $P < 0.05$).

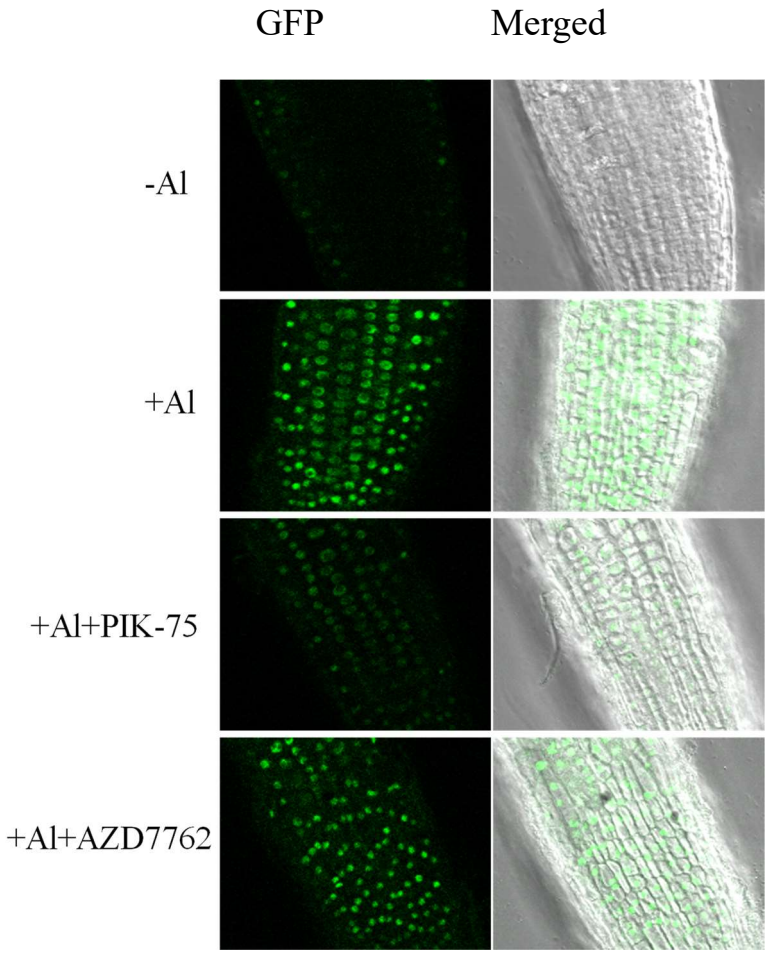

Figure 13. Fluorescence in roots of transgenic Arabidopsis carrying *STOP1* promoter:STOP1-GFP were observed by using LSM-710 leaser-scanning confocal microscope (Carl Zeiss, Tokyo, Japan). Five days old seedlings were incubated in Al-containing medium (10 μM $AlCl_3$, pH5.5) in the presence or absence (+Al as control) of inhibitor for 6 h [All treatments contain the same concentration of DMSO (0.1%)].

II
Involvement of Lipid Signals in Early Al-inducible Malate Secretion in *Arabidopsis thaliana*

ABSTRACT

Phosphatidylinositol metabolism is known to be involved in multiple biological processes, such as lipid homeostasis, vesicular trafficking, and membrane-bound regulators of signaling proteins. In this study, specific-inhibitory assays were performed to investigate whether lipid signals participate in Al-responsive malate secretion or not. These specific inhibitors included PI4K-specific/PI3K-specific/PLC-specific (PAO, LY294002, and U73122, respectively). Our results revealed that the phosphatidylinositol metabolic pathways differently regulate aluminum-induced malate secretion. Early aluminum-induced transcription of *AtALMT1* and other aluminum-responsive genes was significantly suppressed by phosphatidylinositol 4-kinase (PI4K) and phospholipase C (PLC) inhibitors, indicating that the PI4K-PLC metabolic pathway activates early aluminum-signaling. Inhibitors of phosphatidylinositol 3-kinase (PI3K) and PI4K reduced aluminum-activated malate transport by AtALMT1, suggesting that both the PI3K and PI4K metabolic pathways regulate this process. These results were validated using T-DNA insertion mutants of *PI4K* and *PI3K*-RNAi lines. We also found a reduction of aluminum-induced citrate secretion in tobacco by applying inhibitors of PI3K and PI4K. Taken all, our results indicated that phosphatidylinositol metabolism regulates organic acid secretion in plants under aluminum stress.

1. INTRODUCTION

The hydrolysis of phosphatidylinositol 4,5-bisphosphate [PI(4,5)P_2] into inositol 1,4,5-trisphosphate (IP_3) and *sn*-1,2-diacylglycerol (DAG) that catalyzed by phospholipase C (PLC) is known to be final step of phosphatidylinositol (PtdIns) metabolism. These reactions have been considered to be a lipid second messenger to distinct roles of signal transduction in plants. Firstly, IP_3 binds to a membrane receptor, a ligand-gated Ca^{2+} channel, releasing Ca^{2+} into the cytoplasm then to regulate cell proliferation and other cellular reactions that require free calcium. Secondly, DAG activates protein kinase C to convert DAG to phosphatidic acid (PA) (Berridge, 1993; Arisz et al., 2009). In Arabidopsis, two types of PLCs are identified as: non-specific PLC (NPC) and phosphoinositide-specific PLC (PI-PLC). The former one representatives the enzymes that hydrolyzes lots of phospholipids, while the PI-PLC is specific to PI(4,5)P_2 and its related derivatives (Nakamura et al., 2005). Kanehara et al. (2015) found that AtPLC2 is the primary phospholipase in PtdIns metabolism and both regulates the seedlings growth and responses to endoplasmic reticulum (ER) stress in *Arabidopsis thaliana*.

PtdIns metabolism regulates multiple biological processes in plants. For instance, Kim et al. (2001) suggested that PI4K involved in the PI3P-dependent trafficking from the trans-Golgi network to the prevacuolar compartment. Furthermore, inhibitory assays indicated that PI4K contributes to the internalization of CESA3 (cellulose synthase 3) from plasma membrane (PM) at the early step of endocytosis, meanwhile PI3K involves in the intercellular transport of CESA3 from Golgi apparatus to PM (Fujimoto et al., 2014). These discoveries strongly suggest that PI4K and PI3K display important and distinct roles in intercellular signaling transduction, including membrane trafficking. In yeast, animal and plant cells, the first step in the initiation of endocytosis requires activation of PI3K (Kim et al., 2001). More recently, Takahashi et al. (2017) found that treatment with PI4K inhibitor PAO specifically inhibited the stomatal response to CO_2, while PI3K inhibitor LY294002 specifically inhibited the stomatal response to darkness compared with that to CO_2 and abscisic acid (ABA), indicated that PI4K and PI3K play a critical role in the CO_2 and darkness signal transduction pathway, respectively. PtdIns

metabolism has been implicated in the response to other environment stimuli such as pathogen (Van der Luit *et al.*, 2000; Laxalt and Munnik, 2002), drought (Mane *et al.*, 2007; Wang *et al.*, 2008; Liu *et al.*, 2013), and ABA response (Sanchez and Chua, 2001; Hunt *et al.*, 2003; Mills *et al.*, 2004). However, lipid signal interacts with Al-responsive signaling pathway is rarely reported.

In general, lipid signal production is fast (minutes) and transient. Jones and Kochian (1995) found that Al significantly reduced the levels of Ins(1,4,5)P_3 in the wheat root apices which had been pre-incubated with H_2O_2 (10 mM) for stimulated IP_3 when compared with non-Al treatment, suggesting that Al may be interfering with the phosphoinositide signal transduction pathway. Furthermore, the authors also confirmed that Al can caused a dramatic inhibitory effect on PLC activity with increasing concentration of $AlCl_3$. Al may present as a low molecular weight and stable complex Al-citrate in the cytoplasm (Ohman and Martin, 1994). However, Ins(1,4,5)P_3 hydrolysis was not affected by Al-citrate in either the microsomal membrane or the soluble fraction (Jones and Kochian, 1995), suggesting that Al may specifically target PLC, rather than dephosphorylated Ins(1,4,5)P_3. In that study, authors also proposed that Al not only inhibits PLC activity but also inhibits either the synthesis or the availability of PLC substrate, PtdInsP_2, which should be further confirmed. In mammalian, it has been reported that Al toxicity in the neuronal cells may be linked to aberrations in the phosphoinositide-associated signal transduction pathway which resulted in either alterations in Ca^{2+} homeostasis or changes in cytoskeletal dynamics (Macdonald et al., 1987; Nixon et al., 1990; Haug et al., 1994). These findings suggest that there may be a cross-talk between Al-responsive signal and PtdIns metabolism in plants.

In this study, specific-inhibitory assays were performed to investigate whether lipid signals participate in Al-responsive malate secretion or not. These specific inhibitors included PI4K-specific/PI3K-specific/PLC-specific (PAO, LY294002, and U73122, respectively). Our results suggested PtdIns metabolism plays critical roles in early Al-inducible expression and Al-activated malate transport.

2. MATERIAL AND METHODS

Arabidopsis accessions

The following T-DNA insertion mutants of *PI4Kβ2* (*pi4kβ2;* SALK_098069), *PI4Kβ1* (*pi4kβ1;* SALK_040479), *PI4Kα1* (*pi4kα1*, SALK_011790), *PI4Kα2* (At1g51040) (*pi4kα2*; SALK_046774C) were obtained from Nottingham Arabidopsis Stock Centre (NASC). Homozygosity of these lines was confirmed by genomic PCR using primers recommended by the SALK database (Table 1) and they were propagated by the single seed-decent method. We could isolate homozygous lines of *pi4kα1* and *pi4kβ2* as putative targets of PIK-75(Fig. 1). For the preparation of RNAi lines, genomic DNA sequence specific to *PI3K* (region: 138–437 bp) was cloned into the vector pGWB80 of Gateway cloning kit (Invitrogen, Tokyo, Japan) and transformed into Arabidopsis by the *Agrobacterium*-mediated method, as described previously (Kobayashi *et al.*, 2014). Homozygous T_2 transgenic lines of *PI3K*-RNAi were isolated by kanamycin and hygromycin selection (Fig. 1).

Chemical profiling of malate secretion and Al-inducible gene expression

LY294002 (PI3K inhibitor, 25 μM; Walker *et al.*, 2000), phenylarsine oxide (hereafter PAO, PI4K inhibitor, 1 μM; Vermeer *et al.*, 2009), and U73122, U73343 (PLC inhibitor, structural inactive analogue of U73122, 2 μM; Abd-El-Haliem *et al.*, 2016) were used for profiling Al-activated malate transport by AtALMT1 and gene expression.

Root growth assay

Wild-type Col-0 were precultured in a transparent plastic pot (150 mL modified MGRL solution without Pi at pH 5.5) for 4 d as described in chapter 1. For assessing effect of inhibitors on the root growth, 4-day-old seedlings were transferred the Al containing solutions (10 μM Al, without Pi at pH 5.0) in the presence or absence (as control = 100%) of inhibitors (1 μM PAO, 25 μM LY294002, 2 μM U73122, and 2 μM U73343, respectively) for 3 h, then transferred to

the 1/2 MS medium (with 1% sucrose and 1% agar at pH 5.5) for root growth. All experimental operations are carried out in a clean bench. Root elongation was measured at day 3.

Quantification of malate contents of root cells

Malate contents of root cells were quantified with the cell extracts using the same quantification method used for the malate secretion assay. The cell extracts were obtained by grinding the roots (5 to 10 mg) using a disposable pestle in a micro tube containing 100 μl of 0.6 M $HClO_4$, then removing cell debris by centrifugation (2,400 x g for 10 min). The supernatant was used as cell extracts.

The other conditions are same with chapter 1.

3. EXPERIMENTAL RESULTS

3.1 Effects of PI3K and PI4K inhibitors on Al-inducible malate secretion

Because only PIK-75 inhibited both early Al-inducible expression and Al-activated malate transport by AtALMT1, we analyzed the molecular mechanisms underlying Al signaling that is inhibited by PIK-75 further. A homology search identified that both PI3K and PI4Ks of Arabidopsis are highly homologous to human p110α (Table 4). Furthermore, *in silico* binding assay indicated that the homologous PI3K and PI4Ks could bind to PIK-75 at the interacting domain with similar docking score (Fig. 11 in chapter 1). These findings strongly suggest that PIK-75 can inhibit both PI3K and PI4Ks in Arabidopsis; therefore, we used the pharmacological approach to separate the effects of PI3K and PI4K on Al-inducible malate secretion.

Further characterization of PI3K and PI4K inhibitors LY294002 and PAO, which were previously used in plant research, identified that PI3K and PI4K inhibitors blocked Al-responsive events controlled by AtALMT1 differently. PAO significantly inhibited early Al-inducible expression of *AtALMT1* (22%) and other STOP1-regulated genes (*ALS3* and *MATE* reduced to 61% and 67%, respectively), while LY294002 did not show any suppressing effect on these Al-inducible expressions (3 h; Fig. 2). Additionally, PAO also suppressed the early Al-inducible expression of Al-biomarker genes. In contrast, LY294002 did not inhibit Al-inducible expression of these genes, except for one of the Al-biomarker genes *At5g13320* (3 h; Fig. 3). These results strongly suggest that metabolites derived from the PI4K pathway regulate early Al-inducible expression of *AtALMT1* and several other genes.

We further analyzed the Al-activated malate secretion using the 35S:*AtALMT1* (constitutively expresses *AtALMT1*) to evaluate the effect of these inhibitors on the process of Al-activated malate transport. We found that PAO and LY294002 reduced malate secretion to 21% and 59%, respectively by the 35S:*AtALMT1* plants (2 h; Fig. 4). In contrast, we did not find any reduction of malate content of the root cells by these inhibitors (Fig. 5). This suggested that PI3K and PI4K inhibitors inhibit the process of Al-activated malate transport but not the

synthesis of malate.

3.2 Effects of PLC inhibitor on Al-inducible malate secretion

PLC acts downstream of the PI4K-mediated pathway, but not downstream of PI3K (Delage *et al.*, 2012). We examined the effects of PLC inhibitor U73122 and its structural inactive analog U73343 (as a negative control; Abd-El-Haliem *et al.*, 2016) on early Al-inducible expression in wild-type (e.g. 3 h) and malate transport in 35S:*AtALMT1* (e.g. 2 h). Al-inducible expression of STOP1-regulated genes (*AtALMT1*, *ALS3*, and *MATE* decreased to 23%, 24%, and 54%, respectively), as well as Al-biomarker genes, were significantly suppressed by U73122, but not by U73343 (Fig. 6). It indicates that metabolites derived from the PLC pathway are critical for early Al-inducible expression.

On the other hand, Al-activated malate transport in 35S:*AtALMT1* was suppressed slightly by U73122 (85% and 94% by U73122 and U73343, respectively; Fig. 7), which was less effective than the PI4K inhibitor PAO (21%; Fig. 4). It suggests that PI4K-mediated pathway is more essential for Al-activated malate transport than PLC-mediated pathway. Additionally, the PI3K-mediated pathway also plays an important role in the Al-activated process because malate transport in 35S:*AtALMT1* was suppressed significantly by LY294002 as showed in figure 4.

3.3 Effect of PI3K and PI4K inhibitors on Al-inducible citrate secretion in tobacco (*Nicotiana tabacum*)

As described, Al-inducible expression of STOP1-regulated genes *AtALMT1*, *ALS3*, and *MATE* in Arabidopsis is regulated by metabolites derived from the PI4K, but not the PI3K, pathway (Fig. 2). To evaluate whether this is a ubiquitous regulatory mechanism that the expression is regulated by STOP1-like proteins among higher plants, we tested the effect of PI4K and PI3K inhibitors PAO and LY294002 on *NtMATE* expression in 30 μM Al-containing medium for 6 h. Our previous study has indicated that Al-inducible expression of *NtMATE* is controlled by NtSTOP1 (Ohyama *et al.*, 2013). Assays assessing inhibition showed that PAO

significantly inhibited the expression of *NtMATE* (32%), while LY294002 did not, compared with that under Al conditions (100%; Fig. 8A). On the other hand, citrate secretion in tobacco roots was significantly suppressed by both PI4K and PI3K inhibitors (38% and 76%, respectively; Fig. 8B) compared with that under Al conditions (100%), suggesting the involvement of the PI3K- and PI4K-mediated pathways in the Al-inducible citrate secretion in tobacco.

3.4 Effects of PI3K, PI4K, and PLC inhibitors on transcription of *CAMTA2* and *WRKY46*

As described, both PIK-75 and AZD7762 can inhibit the late-phase (e.g. 24 h) *AtALMT1* expression (Fig. 5 in chapter 1); however, PIK-75 can also inhibit PI3K and PI4Ks in Arabidopsis (Table 4 and Fig. 11 in chapter 1). We propose that either PI3K or PI4K involves in Al-inducible *AtALMT1* expression in the late phase of treatment. Since transcription factors CAMTA2 (activator of *AtALMT1*) and WRKY46 (repressor; Ding *et al.*, 2013) regulate Al-inducible *AtALMT1* expression in the late phase of treatment (Tokizawa *et al.*, 2015), we further profiled effects of PI4K and PI3K inhibitors PAO and LY294002, as well as PLC inhibitor U73122, on expression of *CAMTA2* and *WRKY46*.

We found that both PAO and U73122, but not LY294002, significantly inhibited expression of *CAMTA2* (expression was reduced to 0.1 and 0.42 by PAO and U73122, respectively), but upregulated *WRKY46* (expression was upregulated to 2.51 and 8.02 by PAO and U73122, respectively), compared with no-inhibitor condition (control = 1) after cotreatment with Al for 24 h (Fig. 9). These results indicate that metabolites derived from PI4K- and PLC-mediated pathways modulate CAMTA2 and WRKY46 to regulate the late phase of Al-inducible *AtALMT1* expression.

3.5 Characterization of Al-inducible malate secretion in the roots of *PI3K*-RNAi and *PI4K* T-DNA insertion mutants

To validate the role of PI3K and PI4K metabolic pathways in the regulation of Al-inducible

malate secretion as suggested by our pharmacological assays, we analyzed *AtALMT1* expression and malate release in the available T-DNA insertion mutants, *pi4kα1* and *pi4kβ2*, and in the *PI3K*-RNAi transgenic lines, prepared by us. Both the Al-inducible expression of *AtALMT1* and malate secretion were suppressed in the roots of *pi4kα1* and *pi4kβ2*, compared with wild-type (Fig. 10A, C). However, knockdown of *PI3K* by RNAi did not affect the expression of *AtALMT1* but significantly suppressed malate secretion (Fig. 10B, D). The suppression of Al-induced malate secretion was greater in *pi4kβ2* and *PI3K*-RNAi line #5 than the other two mutants; meanwhile, the growth of primary roots of these two mutants (e.g. *pi4kβ2* and *PI3K*-RNAi line #5) was significantly inhibited by Al treatment, compared to that of the wild-type (Fig. 11). This supported our hypothesis that both PI3K and PI4K metabolic pathways contribute to Al tolerance by regulating malate secretion.

4. DISCUSSION

PIK-75 is known to specific-inhibit human p110α, isoform of PI3K (Zheng et al., 2011). However, *in silico* binding assays showed that PIK-75 could bind to both PI4K and PI3K in *Arabidopsis thaliana*. Based on the 'UniProt' database and 'BLAST' (Basic Local Alignment Search Tool) analysis, five putative Arabidopsis proteins were identified that having high homology to PI3K in *Homo sapiens (Human)*, including At1g49340 (AtPI4Kα1), At1g60490 (PI3K), At1g51040 (AtPI4Kα2), At5g09350 (AtPI4Kβ2), and At5g64070 (AtPI4Kβ1) (Table 4 in chapter 1). These findings suggest that both PI4K and PI3K are responsible for malate secretion in response to Al treatment. In fact, specific-inhibitory assays of PI4K and PI3K inhibitors further supported our hypothesis.

There is a dearth of information about PtdIns-signals in plants under Al stress. Jones and Kochian (1995; 1997) previously reported that PtdIns metabolism pathway may involve in early Al signaling; however, its relationship to Al-inducible malate secretion has not been clarified. In the current study, PI4K inhibitor PAO as well as T-DNA mutants of *PI4K*, but neither PI3K inhibitor LY294002 nor *PI3K*-RNAi lines, suppressed Al-inducible expression of STOP1-regulated genes and Al-biomarker genes (Fig. 2, 3 and 10), suggesting that signaling lipids produced from PI4K-mediated pathway participate in early Al-inducible expression of multiple genes, including Al-tolerant genes. Furthermore, our root growth assay of wild-type Arabidopsis after 3 h cotreatment with Al and the inhibitors showed that PI4K inhibitor PAO enhanced its Al sensitivity (Fig. 12). This could account for the suppressing effect of PAO on Al-inducible expression of multiple Al-tolerant genes (Fig. 2).

PLC, which acts downstream of the PI4K-mediated pathway (Delage *et al.*, 2012) and responses to early environmental stress (Ruelland *et al.*, 2002), hydrolyzes phospholipids to diacylglycerol (DAG) and inositol 1,4,5-trisphosphate (IP_3) (Munnik *et al.*, 1996; Fig. 13). We investigated whether metabolites derived from the PLC pathway are involved in early Al-responsive signaling transduction or not further. We observed that U73122 (PLC inhibitor), but not U73343 (an inactive analog of U73122), significantly inhibited Al-inducible expression of

all tested genes (e.g. STOP1-regulated genes and Al-biomarker genes; Fig. 6). This strongly suggests that metabolites derived from the PLC pathway are critical for early Al-responsive signaling transduction (Fig. 14). This hypothesis is further supported by the results of the root growth assay with PLC inhibitor U73122 which enhanced the Al sensitivity of root tips of wild-type (Fig. 12). This is in accordance with the previous findings that IP_3 transiently increases in cultured coffee (*Coffea arabica*) cells under Al stress (Poot-Poot and Teresa Hernandez-Sotomayor, 2011).

Al-activated malate secretion in 35S:*AtALMT1* (2 h; Fig. 4), but not the malate content of the root cells of Arabidopsis (Fig. 5) was significantly suppressed by PI3K and PI4K inhibitors LY294002 and PAO, suggesting that PtdIns metabolism is responsible for the activation of malate transport by AtALMT1. The reduction of malate secretion, but not *AtALMT1* expression, in the *PI3K*-RNAi lines also supports this hypothesis (Fig. 10B, D). Furthermore, the T-DNA insertion mutants of *PI4K* showed about 50% reduction of malate secretion but only 20% suppression of *AtALMT1* expression, suggesting a role of PI4K in the activation of the AtALMT1 protein (Fig. 10A, C). However, PLC inhibitor U73122 slightly reduced malate secretion in 35S:*AtALMT1* (Fig. 7), suggesting that the PLC-mediated pathway is less contributing to the activation of malate transport. There are several possible mechanisms of regulation of Al-activated malate transport by the PI3K- and PI4K-mediated pathways. Previous studies have identified the involvement of PI3K and PI4K in different steps of intracellular trafficking (Li *et al.*, 1995; Kim *et al.*, 2001). For example, PI3K was suggested to play a direct role in vesicular transport from Golgi to the vacuole (Stack *et al.*, 1995), while PtdIns4P is essential for transport from Golgi to the PM in yeast (Hama *et al.*, 1999). In Arabidopsis, internalization of CESA3 (cellulose synthase 3) from the PM is mediated by PI4K, while PI3K is an essential element for CESA3 transport from the Golgi to the PM (Fujimoto *et al.*, 2014). Hence, it is possible that regulation of AtALMT1 protein transport to the PM can be similarly controlled by PI3K and PI4K. Another possibility is that the different phosphoinositide derivatives from the PI3K- and PI4K-metabolic pathways (e.g. PtdIns4P,

PtdIns(4,5)P_2, and PtdI5P), localizing primarily at the PM (Vermeer *et al.*, 2009), are essential for activating the malate transporter (Fig. 14). The hypothesis of activation of OA-transporters under Al stress by PI3K is further supported by our experiments in a different species of tobacco. *NtMATE* expression was not inhibited but citrate release was reduced by the PI3K inhibitor LY294002 (Fig. 8).

Furthermore, we also observed that both PI4K and PLC inhibitors PAO and U73122 suppressed *CAMTA2* expression, but significantly activated *WRKY46* after long-term treatment with Al (e.g. 24 h; Fig. 9). It indicates that PLC-mediated pathway (e.g. IP_3, PA) regulates the late phase of Al-inducible expression of *AtALMT1* through transcription factors CAMTA2 and WRKY46. These signaling lipids might act upstream of CIPKs/CDPKs in Al-responsive *AtALMT1* expression as PA reportedly activates CDPKs in plants (Farmer and Choi, 1999) and *CAMTAs* expression is regulated by downstream of PI4K pathway (Arabidopsis, Doherty *et al.*, 2009; barley, Gierczik *et al.*, 2017). Taken all, our results indicate that not only PtdIns metabolism but also calcium signaling play important roles in the transcriptional regulation of *AtALMT1* (Fig. 14).

In conclusion, we uncover that PtdIns metabolism plays critical roles in early Al-inducible expression and Al-activated malate transport (Fig. 14). We identified that PI3K- and PI4K-mediated PtdIns metabolism interferes with the process of Al-activated malate transport. However, the PLC-mediated pathway is critical for early Al-inducible expression of various Al-tolerance genes (e.g. *AtALMT1*, *ALS3*, *MATE*) and Al-biomarker genes. These signaling lipids may act upstream of CIPKs/CDPKs to regulate late-phase *AtALMT1* expression. Because similar inhibitory effects were observed in tobacco (Fig. 8), we could infer that PtdIns metabolism plays critical roles in Al-tolerance mechanisms in various plants. However, PtdIns metabolism has been implicated in the response to other environment stimuli apart from Al, such as pathogen (Van der Luit *et al.*, 2000; Laxalt and Munnik, 2002), drought (Mane *et al.*, 2007; Wang *et al.*, 2008; Liu *et al.*, 2013), and ABA response (Sanchez and Chua, 2001; Hunt *et al.*, 2003; Mills *et al.*, 2004). This suggests that the central hub of signaling, PtdIns

metabolism can interact with other signal transducers in response to different stresses (Ruelland *et al.*, 2015). This is further supported by a recent RNAseq study, which hypothesized the involvement of G-proteins in activating PtdIns metabolic pathway upstream to *MATE* in *Stylosanthes* under Al stress (Jiang *et al.*, 2018). Furthermore, we identified several receptor-type tyrosine kinases that inhibited malate secretion, which can couple with G-proteins (Table 3 in chapter 1). Further characterization of these inhibitors would be useful for identifying unknown receptor proteins that are involved in the Al-responsive signal transduction pathways.

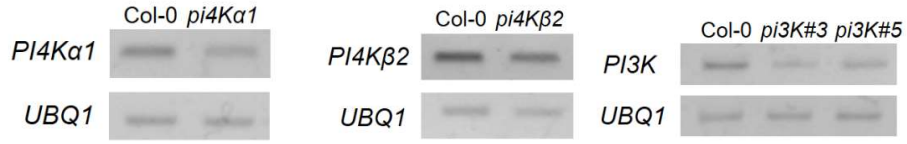

Figure 1. Reverse transcription-polymerase chain reaction (RT-PCR) analysis of gene transcripts for *PI4Kα1* (*At1g49340*), *PI4Kβ2* (*At5g09350*), and *PI3K* (*At1g60490*) in wild-type and mutants. Roots of the 10-day-old seedlings of wild-type Col-0 and mutants (*PI4K* T-DNA insertion mutants: *pi4kα1* and *pi4kβ2*; *PI3K*-RNAi transgenic lines: *pi3k*) were exposed to the Al containing solutions (10 μM $AlCl_3$ at pH 5.0) for 6 h. *UBQ1* (*At3g52590*) was used as a positive control. Primers specific for *UBQ1* (Forward: TCGTAAGTACAATCAGGATAAGATG; Reverse: CACTGAAACAAGAAAAACAAACCCT), *PI4Kα1* (Forward: CCGAGGAAATGGAAATGAGA; Reverse: GCCACAGCAAGCAAATAGGT), *PI4Kβ2* (Forward: TTGAAATTGGTCTGGATTCG; Reverse: CAATGAAAGAAACTGTGCCATC), and *PI3K* (Forward: GGGGATTGTGGCAGGAGAA; Reverse: TGAACCCGCCATGAGATGAA) were used for RT-PCR analysis.

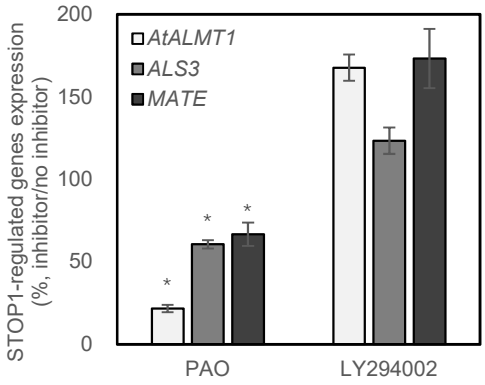

Figure 2. Effects of inhibitors on the Al-inducible expression of STOP1-regulated genes. Using the same experimental conditions as in figure 5 of chapter 1, the effects of PI4K (1 μM PAO) and PI3K (25 μM LY294002) inhibitors on early (3 h) Al-inducible expression of STOP1-regulated genes in wild-type were analyzed. The asterisks in each treatment represent significant differences compared with no inhibitor control (100%) (LSD test; *, $P < 0.05$). The mean ± SD values of the three replicates are shown.

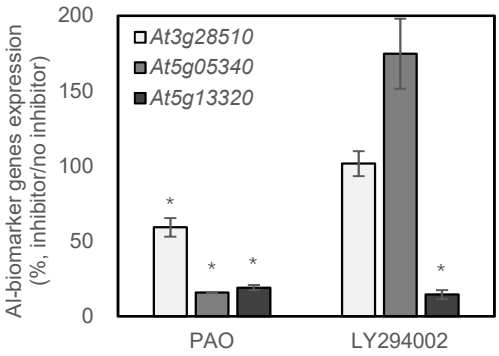

Figure 3. Effects of inhibitors on the Al-inducible expression of Al-biomarker genes. Using the same experimental conditions as in figure 5 of chapter 1, the effects of PI4K (1 μM PAO) and PI3K (25 μM LY294002) inhibitors on early (3 h) Al-inducible expression of Al-biomarker genes in wild-type were analyzed. The asterisks in each treatment represent significant differences compared with no inhibitor control (100%) (LSD test; *, $P < 0.05$). The mean ± SD values of the three replicates are shown.

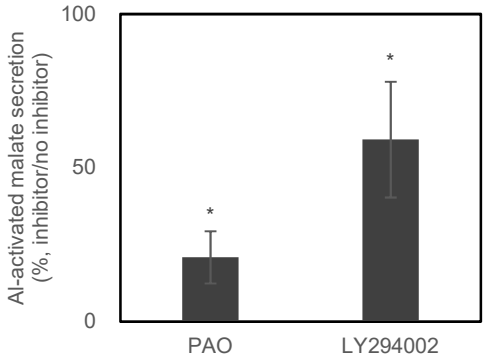

Figure 4. Effects of inhibitors on the Al-activated malate secretion. Using the same experimental conditions as in figure 4 of chapter 1, the effects of PI4K (1 μM PAO) and PI3K (25 μM LY294002) inhibitors on the early Al-activated malate secretion (2 h) in transgenic plants 35S:*AtALMT1* were analyzed. The asterisks in each treatment represent significant differences compared with no inhibitor control (100%) (LSD test; *, $P < 0.05$). The mean ± SD values of the three replicates are shown.

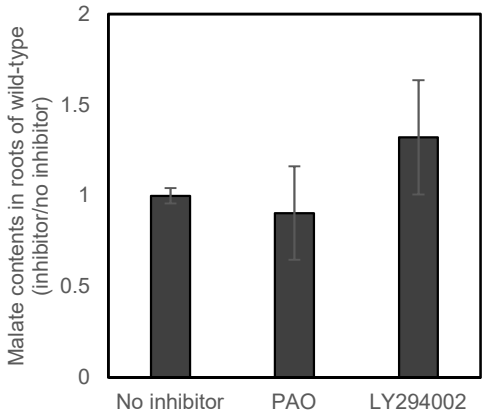

Figure 5. Effect of PI4K (PAO) and PI3K (LY294002) inhibitors on the malate contents of the roots of wild-type. Seedlings were precultured in a transparent plastic pot (150 mL modified MGRL solution without Pi at pH 5.5) for 4 d as described in the materials and methods. Four-day-old seedlings (*in vitro* culture) of wild-type Arabidopsis were transferred to solutions (1% sucrose at pH 5.0) in the presence or absence (as control = 1) of inhibitors (1 μM PAO and 25 μM LY294002, respectively) for 6 h. The means of relative malate contents (inhibitor/no inhibitor) ± SD values of the three replicates are shown. (LSD test; *, $P < 0.05$).

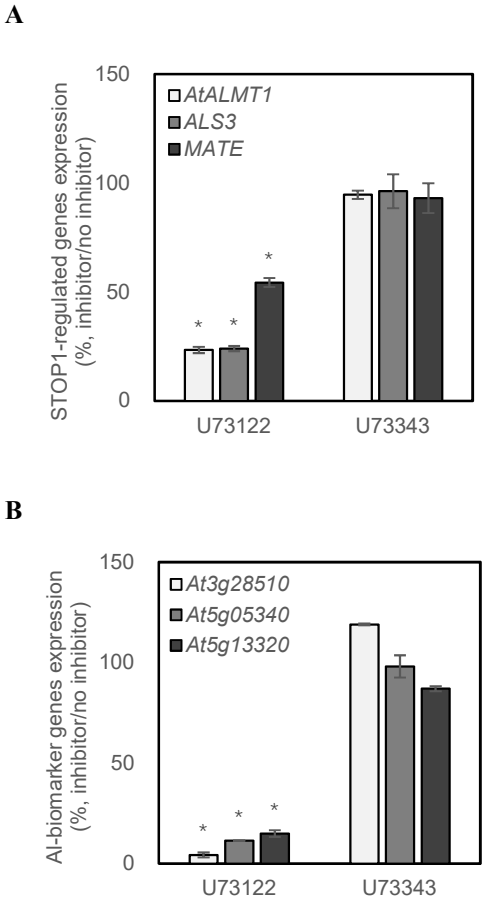

Figure 6. Effect of PLC inhibitor on the expression of STOP1-regulated genes and Al-biomarker genes in the roots of wild-type. Using the same experimental conditions as in figure 5 of chapter 1, the effects of PLC inhibitor U73122 (2 μM) and its structural inactive analog U73343 on early (3 h) Al-inducible expression of STOP1-regulated genes (**A**) and Al-biomarker genes (**B**) in wild-type were analyzed. The asterisks in each treatment represent significant differences compared with the no inhibitor control (100%) (LSD test; *, $P < 0.05$). The mean ± SD values of the three replicates are shown.

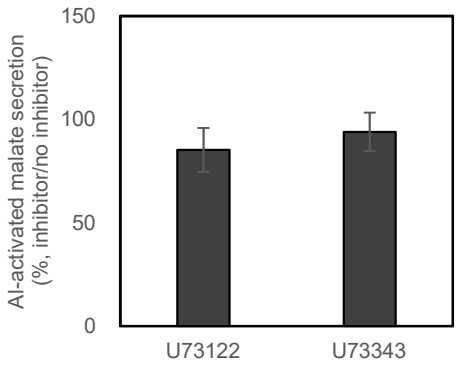

Figure 7. Effect of PLC inhibitor on the Al-activated malate transport in the roots of transgenic plants 35S:*AtALMT1*. Using the same experimental conditions as in figure 4 of chapter 1, the effects of PLC inhibitor U73122 (2 μM) and its structural inactive analog U73343 on early Al-activated malate secretion (2 h) in transgenic plants 35S:*AtALMT1* were analyzed. The asterisks in each treatment represent significant differences compared with the no inhibitor control (100%) (LSD test; *, $P < 0.05$). The mean ± SD values of the three replicates are shown.

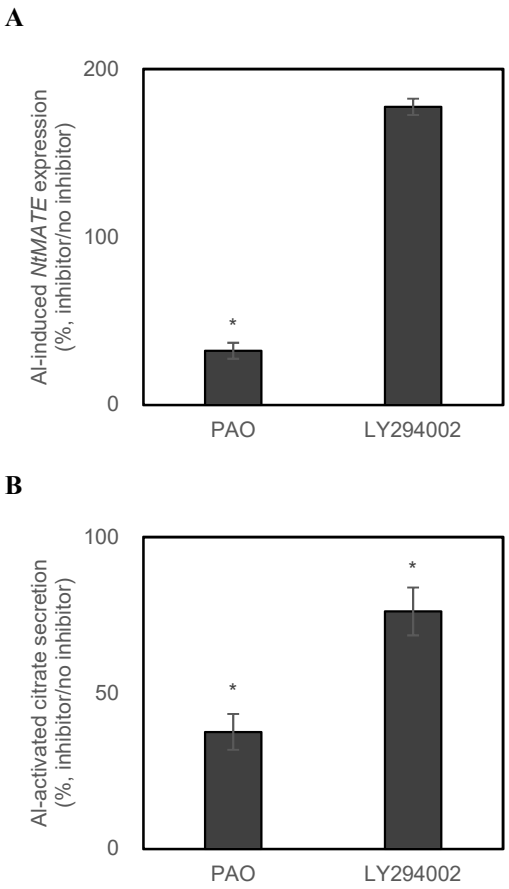

Figure 8. *NtMATE* expression and citrate secretion in the root apexes of tobacco under cotreatment with Al and inhibitors. (**A**) The relative expression level of *NtMATE* in the roots of tobacco. Ten-day-old seedlings were exposed to either 30 μM $AlCl_3$ (as a control = 100%) or medium containing both Al and inhibitor for 6 h. *NtMATE* expression was quantified using quantitative real-time RT-PCR with *NtActin* as an internal control (*NtMATE*/*NtActin*). (**B**) Relative citrate secretion in the root apexes of tobacco. Five-day-old seedlings were exposed to either 30 μM $AlCl_3$ (as a control = 100%) or medium containing both Al and inhibitor for 24 h. The final concentration of each inhibitor was 1 μM PAO (PI4K inhibitor) and 25 μM LY294002 (PI3K inhibitor). The asterisks in each treatment represent significant differences compared with no inhibitor control (100%) (LSD test; *, $P < 0.05$). The mean ± SD values of the three replicates are shown.

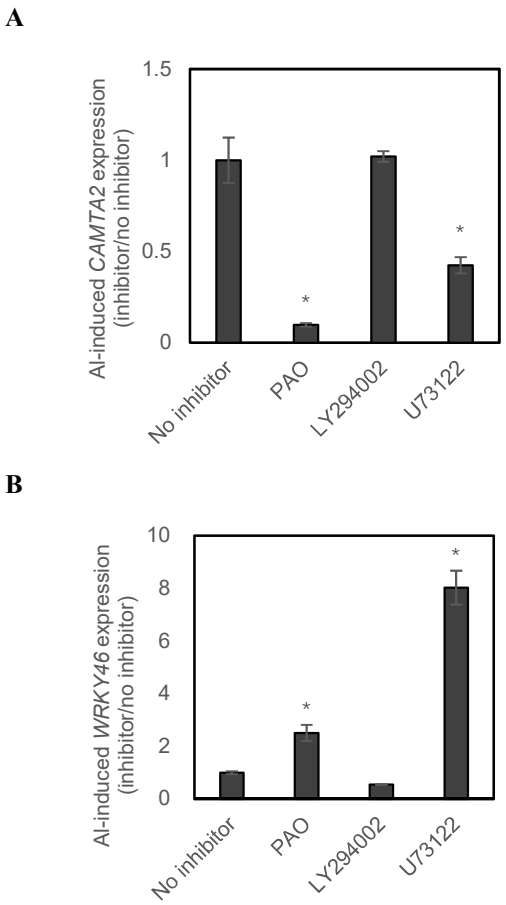

Figure 9. Effects of inhibitors (PAO, LY294002, and U73122) on the expression levels of *CAMTA2* and *WRKY46* in the roots of wild-type. Using the same experimental conditions as in figure 5 in chapter 1, the effects of inhibitors PAO (1 μM, PI4K inhibitor), LY294002 (25 μM, PI3K inhibitor), and U73122 (2 μM, PLC inhibitor) on expression levels of *CAMTA2* (activator of *AtALMT1*) (**A**) and *WRKY46* (repressor of *AtALMT1*) (**B**) in wild-type were analyzed. Expression levels of *CAMTA2* and *WRKY46* at 24 h were quantified by quantitative real-time RT-PCR using *UBQ1* as an internal control. The asterisks in each treatment represent significant differences compared with no inhibitor (control = 1) (LSD test; *, $P < 0.05$). The mean ± SD values of the three replicates are shown.

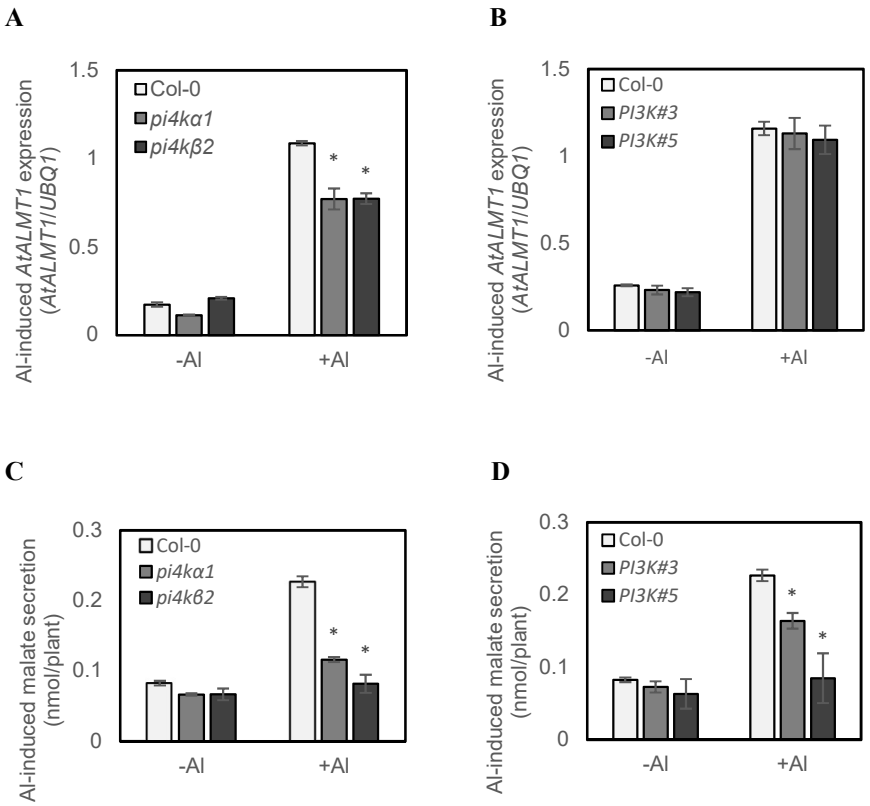

Figure 10. Al-responsive *AtALMT1* expression and malate secretion in *PI4K* T-DNA insertion mutants (*pi4kα1* and *pi4kβ2*) and *PI3K*-RNAi transgenic lines. Roots of the 10-day-old seedlings of *PI4K* mutants and *PI3K*-RNAi lines were exposed to modified MGRL medium in the presence or absence (as control) of 10 μM $AlCl_3$ at pH 5. *AtALMT1* expression levels in the roots of *PI4K* knockout mutants (**A**) and *PI3K*-RNAi lines (**B**) after exposing to either 0 μM Al or 10 μM Al-containing medium for 6 h. *AtALMT1* expression levels were quantified by quantitative real-time RT-PCR using *UBQ1* as an internal control. Malate secretion from four-day-old seedlings (*in vitro* culture) of *PI4K* mutants (**C**) and *PI3K*-RNAi lines (**D**) were analyzed after incubating in the Al-containing solutions (10 μM Al) for 6 h. The means ± SD values of the three replicates are shown. Asterisks in each treatment represent significant differences compared with wild-type (LSD test; *, $P < 0.05$).

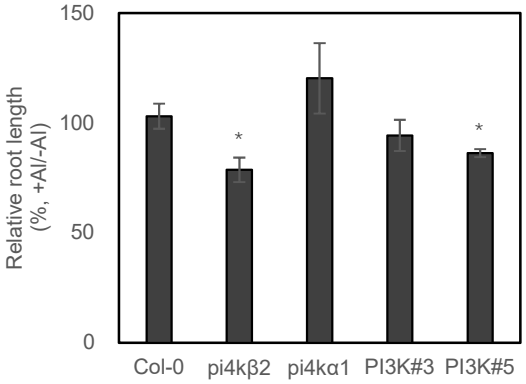

Figure 11. Primary root growth of *PI4K* T-DNA insertion mutants (*pi4kα1* and *pi4kβ2*) and *PI3K*-RNAi transgenic lines. Seedlings of *PI4K* mutants and *PI3K*-RNAi lines were growth in modified MGRL medium in the presence or absence (as control) of 2 μM $AlCl_3$ at pH 5. Relative root growth of *PI4K* mutants and *PI3K*-RNAi lines was measured after incubating in the solutions containing either 0 μM Al or 2 μM Al for 5 days. Five of the 10 seedlings with the longest roots are used to calculate the relative root elongation. Values are means ± SD (n = 5). Asterisks in each treatment represent significant differences compared with wild-type (LSD test; *, $P < 0.05$).

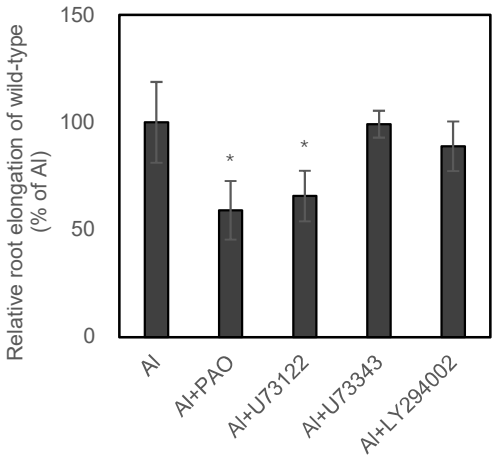

Figure 12. Effects of the inhibitors on the root growth of wild-type under cotreatment with Al. Seedlings were precultured in a transparent plastic pot (150 mL modified MGRL solution without Pi at pH 5.5) for 4 d as described in the materials and methods. For assessing effect of inhibitors on the root growth, 4-day-old seedlings were transferred the Al containing solutions (10 μM Al, without Pi at pH 5.0) in the presence or absence (as control = 100%) of inhibitors (1 μM PAO, 25 μM LY294002, 2 μM U73122, and 2 μM U73343, respectively) for 3 h, then transferred to the 1/2 MS medium (with 1% sucrose and 1% agar at pH 5.5) for root growth. All experimental operations are carried out in a clean bench. Root elongation was measured at day 3. Five of the 10 seedlings with the longest roots are used to calculate the relative root elongation. Values are means ± SD (n = 5).

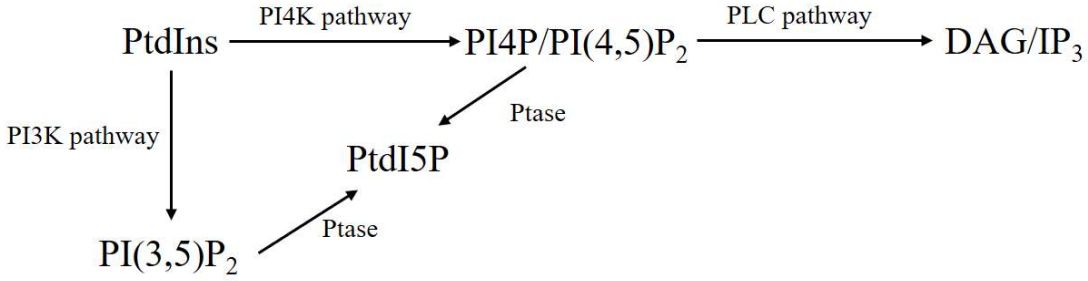

Figure 13. Schematic representation of phosphoinositide metabolic pathways in Arabidopsis. PtdIns, phosphatidylinositol; PI3K, PtdIns 3-kinase; PI4K, PtdIns 4-kinase; PI4P, PtdIns 4-phosphate; $PI(4,5)P_2$, PtdIns 4,5-bisphosphate; $PI(3,5)P_2$, PtdIns 3,5-bisphosphate; PtdI5P, PtdIns 5-phosphate; Ptase, phosphoinositide phosphatase; PLC, phospholipase C; DAG, *sn*-1,2-diacylglycerol; IP_3, inositol 1,4,5-trisphosphate.

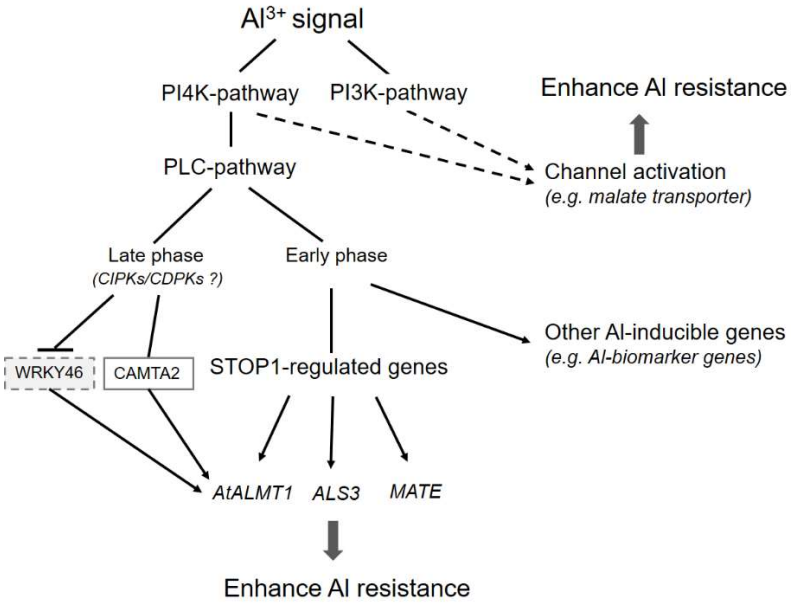

Figure 14. Schematic representation of signal transduction pathways involves in Al-inducible malate secretion in *Arabidopsis thaliana*. Metabolites derived from PLC-mediated pathway regulate both early Al-inducible expression, such as STOP1-regulated genes (e.g. *AtALMT1*, *ALS3*, and *MATE*) and Al-biomarker genes, and late phase of *AtALMT1* expression. Additionally, CIPKs/CDPKs, which may act downstream of PI4K and PLC pathways, regulate the late phase of Al-responsive *AtALMT1* expression by inactivating WRKY46 and/or activating CAMTA2. On the other hand, PI3K and PI4K could involve in the membrane trafficking and localization of the ALMT1 protein or the different phosphoinositide derivatives from the PI3K and PI4K metabolic pathways are essential for activating the malate transporter in the post-translational level. PI3K, PtdIns 3-kinase; PI4K, PtdIns 4-kinase; PLC, phospholipase C; CIPKs, calcineurin B-like protein (CBL)-interacting protein kinases; CDPKs, calcium-dependent protein kinases; Al-biomarker genes, *At3g28510*, *At5g05340*, and *At5g13320*; The black arrows represent Al-responsive signal transduction pathways, while the dotted line represents the activation of malate transporter. The black short line represents suppressing effect.

ACKNOWLEDGMENTS

There is a saying that before the age of 30, you must follow a boss and do your best to improve yourself. I feel so lucky to study in Gifu University. My deepest appreciation to Professor Koyama, who gives me patience, encouragement, knowledge and a lot of opportunity to study under his guidance. My sincere appreciation to Associate Professor Kobayashi and Yamamoto, who give me lots of help in either my study or life. I also would like to thank my lab mates (Tokizawa, Kusunoki, Nakano, Enomoto, Ito, Fujii, Kawai, Huang, Raj, Osawa and so on), who taught me experimental methods and details that help a lot.

Finally, I deeply appreciate my parents and my husband. Their selfless supporting and understanding are indispensable for me to complete this study.

REFERENCES

Abd-El-Haliem AM, Vossen JH, van Zeijl A, Dezhsetan S, Testerink C, Seidl MF, Beck M, Strutt J, Robatzek S, Joosten MH. 2016. Biochemical characterization of the tomato phosphatidylinositol-specific phospholipase C (PI-PLC) family and its role in plant immunity. Biochimica et Biophysica Acta (BBA)-Molecular and Cell Biology of Lipids **1861**(9), 1365–1378.

Alaimo PJ, Shogren-Knaak MA, Shokat KM. 2001. Chemical genetic approaches for the elucidation of signaling pathways. Current Opinion in Chemical Biology **5**(4), 360–367.

Arisz SA, Testerink C, Munnik T. 2009. Plant PA signaling via diacylglycerol kinase. Biochimica et Biophysica Acta (BBA)-Molecular and Cell Biology of Lipids **1791**(9), 869–875.

Balzergue C, Dartevelle T, Godon C, *et al.* 2017. Low phosphate activates STOP1-ALMT1 to rapidly inhibit root cell elongation. Nature Communications **8**, 15300.

Berridge MJ. 1993. Inositol trisphosphate and calcium signalling. Nature **361**(6410), 315.

Bhalla PL. 2006. Genetic engineering of wheat–current challenges and opportunities. TRENDS in Biotechnology **24**(7), 305–311.

Brown LA, O'Leary-Steele C, Brookes P, Armitage L, Kepinski S, Warriner SL, Baker A. 2011. A small molecule with differential effects on the PTS1 and PTS2 peroxisome matrix import pathways. The Plant Journal **65**(6), 980–990.

Burke JE, Inglis AJ, Perisic O, Masson GR, McLaughlin SH, Rutaganira F, Shokat KM, Williams RL. 2014. Structures of PI4KIIIβ complexes show simultaneous recruitment of Rab11 and its effectors. Science **344**(6187), 1035–1038.

Bustin SA, Benes V, Garson JA, *et al.* 2009. The MIQE guidelines: minimum information for publication of quantitative real-time PCR experiments. Clinical Chemistry **55**(4), 611–622.

Daspute AA, Kobayashi Y, Panda SK, Fakrudin B, Kobayashi Y, Tokizawa M, Iuchi S, Choudhary AK, Yamamoto YY, Koyama H. 2018. Characterization of CcSTOP1; a C2H2-type transcription factor regulates Al tolerance gene in pigeonpea. Planta **247**(1), 201–214.

Delage E, Ruelland E, Guillas I, Zachowski A, Puyaubert J. 2012. Arabidopsis type-III phosphatidylinositol 4-kinases β1 and β2 are upstream of the phospholipase C pathway triggered by cold exposure. Plant and Cell Physiology **53**(3), 565–576.

Ding ZJ, Yan JY, Xu XY, Li GX, Zheng SJ. 2013. WRKY 46 functions as a transcriptional repressor of *ALMT1*, regulating aluminum-induced malate secretion in Arabidopsis. The

Plant Journal **76**(5), 825–835.

Doherty CJ, Van Buskirk HA, Myers SJ, Thomashow MF. 2009. Roles for Arabidopsis CAMTA transcription factor in cold-regulated gene expression and freezing tolerance. The Plant Cell **21**(3), 972–984.

Eekhout T, Larsen P, De Veylder L. 2017. Modification of DNA checkpoints to confer aluminum tolerance. Trends in Plant Science **22**(2), 102–105.

Ellman JA. 1996. Design, synthesis, and evaluation of small-molecule libraries. Accounts of Chemical Research **29**(3), 132–143.

Ewan R, Pangestuti R, Thornber S, Craig A, Carr C, O'Donnell L, Zhang C, Sadanandom A. 2011. Deubiquitinating enzymes AtUBP12 and AtUBP13 and their tobacco homologue NtUBP12 are negative regulators of plant immunity. New Phytologist **191**(1), 92–106.

Farmer PK, Choi JH. 1999. Calcium and phospholipid activation of a recombinant calcium-dependent protein kinase (DcCPK1) from carrot (*Daucus carota* L.). Biochimica et Biophysica Acta (BBA)-Protein Structure and Molecular Enzymology **1434**(1), 6–17.

Fujimoto M, Suda Y, Vernhettes S, Nakano A, Ueda T. 2014. Phosphatidylinositol 3-kinase and 4-kinase have distinct roles in intracellular trafficking of cellulose synthase complexes in *Arabidopsis thaliana*. Plant and Cell Physiology **56**(2), 287–298.

Fujiwara T, Hirai MY, Chino M, Komeda Y, Naito S. 1992. Effects of sulfur nutrition on expression of the soybean seed storage protein genes in transgenic petunia. Plant Physiology **99**(1), 263–268.

Gao X, Chen X, Lin W, *et al.* 2013. Bifurcation of *Arabidopsis* NLR immune signaling via Ca^{2+}-dependent protein kinases. PLoS pathogens **9**(1), e1003127.

Gao X, Cox Jr KL, He P. 2014. Functions of calcium-dependent protein kinases in plant innate immunity. Plants **3**(1), 160–176.

Gierczik K, Novák A, Ahres M, *et al.* 2017. Circadian and light regulated expression of CBFs and their upstream signalling genes in barley. International Journal of Molecular Sciences **18**(8), 1828.

Hama H, Schnieders EA, Thorner J, Takemoto JY, DeWald DB. 1999. Direct involvement of phosphatidylinositol 4-phosphate in secretion in the yeast *Saccharomyces cerevisiae*. Journal of Biological Chemistry **274**(48), 34294–34300.

Haug A, Shi B, Vitorello V. 1994. Aluminum interaction with phosphoinositide-associated signal transduction. Archives of Toxicology **68**(1), 1–7.

Hoekenga OA, Maron LG, Piñeros MA, *et al.* 2006. *AtALMT1*, which encodes a malate transporter, is identified as one of several genes critical for aluminum tolerance in

Arabidopsis. Proceedings of the National Academy of Sciences, USA **103**(25), 9738–9743.

Hoekenga OA, Vision TJ, Shaff JE, Monforte AJ, Lee GP, Howell SH, Kochian LV. 2003. Identification and characterization of aluminum tolerance loci in Arabidopsis (Landsberg *erecta*× Columbia) by quantitative trait locus mapping. A physiologically simple but genetically complex trait. Plant Physiology **132**(2), 936–948.

Hoisington D. 2002. Opportunities for nutritionally enhanced maize and wheat varieties to combat protein and micronutrient malnutrition. Food and nutrition bulletin **23**(4), 376–377.

Hunt L, Mills LN, Pical C, Leckie CP, Aitken FL, Kopka J, Roeber BM, McAinsh MR, Hetherington AM, Gray JE. 2003. Phospholipase C is required for the control of stomatal aperture by ABA. The Plant Journal **34**(1), 47–55.

Iuchi S, Koyama H, Iuchi A, Kobayashi Y, Kitabayashi S, Kobayashi Y, Ikka T, Hirayama T, Shinozaki K, Kobayashi M. 2007. Zinc finger protein STOP1 is critical for proton tolerance in *Arabidopsis* and coregulates a key gene in aluminum tolerance. Proceedings of the National Academy of Sciences, USA **104**(23), 9900–9905.

Jiang C, Liu L, Li X, Han R, Wei Y, Yu Y. 2018. Insights into aluminum-tolerance pathways in *Stylosanthes* as revealed by RNA-Seq analysis. Scientific reports **8**(1), 6072.

Jones DL, Kochian LV. 1995. Aluminum inhibition of the inositol 1, 4, 5-trisphosphate signal transduction pathway in wheat roots: a role in aluminum toxicity? The Plant Cell **7**(11), 1913–1922.

Jones DL, Kochian LV. 1997. Aluminum interaction with plasma membrane lipids and enzyme metal binding sites and its potential role in Al cytotoxicity. FEBS Letters **400**(1), 51–57.

Kailasam S, Wang Y, Lo JC, Chang HF, Yeh KC. 2018. S-Nitrosoglutathione works downstream of nitric oxide to mediate iron-deficiency signaling in Arabidopsis. The Plant Journal **94**(1), 157–168.

Kanehara K, Yu CY, Cho Y, Cheong WF, Torta F, Shui G, Wenk MR, Nakamura Y. 2015. Arabidopsis AtPLC2 is a primary phosphoinositide-specific phospholipase C in phosphoinositide metabolism and the endoplasmic reticulum stress response. PLoS genetics **11**(9), e1005511.

Kapuria V, Peterson LF, Fang D, Bornmann WG, Talpaz M, Donato NJ. 2010. Deubiquitinase inhibition by small-molecule WP1130 triggers aggresome formation and tumor cell apoptosis. Cancer research 0008-5472.

Kim DH, Eu YJ, Yoo CM, Kim YW, Pih KT, Jin JB, Kin SJ, Stenmark H, Hwang I. 2001. Trafficking of phosphatidylinositol 3-phosphate from the *trans*-Golgi network to the

lumen of the central vacuole in plant cells. The Plant Cell **13**(2), 287–301.

Kobayashi Y, Hoekenga OA, Itoh H, Nakashima M, Saito S, Shaff JE, Maron LG, Piñeros MA, Kochian LV, Koyama H. 2007. Characterization of *AtALMT1* expression in aluminum-inducible malate release and its role for rhizotoxic stress tolerance in Arabidopsis. Plant Physiology **145**(3), 843–852.

Kobayashi Y, Kobayashi Y, Sugimoto M, Lakshmanan V, Iuchi S, Kobayashi M, Bais HP, Koyama H. 2013a. Characterization of complex regulation of *AtALMT1* expression in response to phytohormones and other inducers. Plant Physiology **162**(2), 732–740.

Kobayashi Y, Kobayashi Y, Watanabe T, Shaff JE, Ohta H, Kochian LV, Wagatsuma T, Kinraide TB, Koyama H. 2013b. Molecular and physiological analysis of Al^{3+} and H^{+} rhizotoxicities at moderately acidic conditions. Plant Physiology **163**(1), 180–192.

Kobayashi Y, Lakshmanan V, Kobayashi Y, Asai M, Iuchi S, Kobayashi M, Bais HP, Koyama H. 2013c. Overexpression of *AtALMT1* in the *Arabidopsis thaliana* ecotype Columbia results in enhanced Al-activated malate excretion and beneficial bacterium recruitment. Plant Signaling & Behavior **8**(9), e25565.

Kobayashi Y, Ohyama Y, Kobayashi Y, *et al.* 2014. STOP2 activates transcription of several genes for Al-and low pH-tolerance that are regulated by STOP1 in *Arabidopsis*. Molecular plant **7**(2), 311–322.

Kochian LV. 1995. Cellular mechanisms of aluminum toxicity and resistance in plants. Annual review of plant biology **46**(1), 237–260.

Lakshmanan V, Kitto SL, Caplan J, Hsueh YH, Kearns D, Wu YS, Bais H. 2012. Microbe-associated molecular patterns-triggered root responses mediate beneficial rhizobacterial recruitment in Arabidopsis. Plant Physiology **160**(3), 1642–1661.

Laxalt AM, Munnik T. 2002. Phospholipid signalling in plant defence. Current opinion in plant biology **5**(4), 332–338.

Letunic I, Bork P. 2017. 20 years of the SMART protein domain annotation resource. Nucleic acids research **46**(D1), D493–D496.

Li G, D'Souza-Schorey C, Barbieri MA, Roberts RL, Klippel A, Williams LT, Stahl PD. 1995. Evidence for phosphatidylinositol 3-kinase as a regulator of endocytosis via activation of Rab5. Proceedings of the National Academy of Sciences, USA **92**(22), 10207–10211.

Li WF, Perry PJ, Prafulla NN, Schmidt W. 2010. Ubiquitin-specific protease 14 (UBP14) is involved in root responses to phosphate deficiency in *Arabidopsis*. Molecular plant **3**(1), 212–223.

Ligaba A, Kochian L, Piñeros M. 2009. Phosphorylation at S384 regulates the activity of the TaALMT1 malate transporter that underlies aluminum resistance in wheat. The Plant Journal **60**(3), 411–423.

Ligaba-Osena A, Fei Z, Liu J, Xu Y, Shaff J, Lee SC, Luan S, Kudla J, Kochian L, Piñeros M. 2017. Loss-of-function mutation of the calcium sensor CBL1 increases aluminum sensitivity in *Arabidopsis*. New Phytologist **214**(2), 830–841.

Liu P, Xu ZS, Pan-Pan L, Hu D, Chen M, Li LC, Ma YZ. 2013. A wheat PI4K gene whose product possesses threonine autophophorylation activity confers tolerance to drought and salt in Arabidopsis. Journal of experimental botany **64**(10), 2915–2927.

Liu Y, Wang F, Zhang H, He H, Ma L, Deng XW. 2008. Functional characterization of the Arabidopsis *ubiquitin-specific protease* gene family reveals specific role and redundancy of individual members in development. The Plant Journal **55**(5), 844–856.

Macdonald TL, Humphreys WG, Martin RB. 1987. Promotion of tubulin assembly by aluminum ion in vitro. Science **236**(4798), 183–186.

Mane SP, Vasquez-Robinet C, Sioson AA, Heath LS, Grene R. 2007. Early PLDα-mediated events in response to progressive drought stress in *Arabidopsis*: a transcriptome analysis. Journal of experimental botany **58**(2), 241–252.

Martínez-Estévez M, Racagni-Di Palma G, Muñoz-Sánchez JA, Brito-Argáez L, Loyala-Vargas VM, Hernandez-Sotomayor T. 2003. Aluminium differentially modifies lipid metabolism from the phosphoinositide pathway in Coffea arabica cells. Journal of Plant Physiology **160**(11), 1297–1303.

Mills LN, Hunt L, Leckie CP, Aitken FL, Wentworth M, McAinsh MR, Gray JE, Hetherington AM. 2004. The effects of manipulating phospholipase C on guard cell ABA-signalling. Journal of experimental botany **55**(395), 199–204.

Munnik T, de Vrije T, Irvine RF, Musgrave A. 1996. Identification of diacylglycerol pyrophosphate as a novel metabolic product of phosphatidic acid during G-protein activation in plants. Journal of Biological Chemistry **271**(26), 15708–15715.

Nakamura Y, Awai K, Masuda T, Yoshioka Y, Takamiya KI, Ohta H. 2005. A novel phosphatidylcholine-hydrolyzing phospholipase C induced by phosphate starvation in Arabidopsis. Journal of Biological Chemistry **280**(9), 7469–7476.

Nishimura T, Hayashi K, Suzuki H, *et al.* 2014. Yucasin is a potent inhibitor of YUCCA, a key enzyme in auxin biosynthesis. The Plant Journal **77**(3), 352–366.

Nixon RA, Clarke JF, Logvinenko KB, Tan MK, Hoult M, Grynspan F. 1990. Aluminum Inhibits Calpain-Mediated Proteolysis and Induces Human Neurofilament Proteins to

Form ProteaseResistant High Molecular Weight Complexes. Journal of neurochemistry **55**(6), 1950–1959.

Ohman LO, Martin RB. 1994. Citrate as the main small molecule binding Al^{3+} in serum. Clinical chemistry **40**(4), 598–601.

Ohyama Y, Ito H, Kobayashi Y, *et al*. 2013. Characterization of *AtSTOP1* orthologous genes in tobacco and other plant species. Plant physiology **162**(4), 1937–1946.

Osawa H, Matsumoto H. 2001. Possible involvement of protein phosphorylation in aluminum-responsive malate efflux from wheat root apex. Plant Physiology **126**(1), 411–420.

Pettersen EF, Goddard TD, Huang CC, Couch GS, Greenblatt DM, Meng EC, Ferrin TE. 2004. UCSF Chimera—a visualization system for exploratory research and analysis. Journal of computational chemistry **25**(13), 1605–1612.

Poot-Poot W, Teresa Hernandez-Sotomayor SM. 2011. Aluminum stress and its role in the phospholipid signaling pathway in plants and possible biotechnological applications. IUBMB Life **63**(10), 864–872.

Rudrappa T, Czymmek KJ, Pare PW, Bais HP. 2008. Root-secreted malic acid recruits beneficial soil bacteria. Plant Physiology **148**(3), 1547–1556.

Ruelland E, Cantrel C, Gawer M, Kader JC, Zachowski A. 2002. Activation of phospholipases C and D is an early response to a cold exposure in Arabidopsis suspension cells. Plant physiology **130**(2), 999–1007.

Ruelland E, Kravets V, Derevyanchuk M, Martinec J, Zachowski A, Pokotylo I. 2015. Role of phospholipid signalling in plant environmental responses. Environmental and Experimental Botany **114**, 129–143.

Ryan PR, Delhaize E, Randall PJ. 1995. Malate efflux from root apices and tolerance to aluminium are highly correlated in wheat. Functional Plant Biology **22**(4), 531–536.

Šali A, Blundell TL. 1993. Comparative protein modelling by satisfaction of spatial restraints. Journal of Molecular Biology **234**(3), 779–815.

Sanchez JP, Chua NH. 2001. Arabidopsis PLC1 is required for secondary responses to abscisic acid signals. The Plant Cell **13**(5), 1143–1154.

Sasaki T, Tsuchiya Y, Ariyoshi M, Ryan PR, Furuichi T, Yamamoyo Y. 2014. A domain-based approach for analyzing the function of aluminum-activated malate transporters from wheat (*Triticum aestivum*) and *Arabidopsis thaliana* in *Xenopus* oocytes. Plant and Cell Physiology **55**(12), 2126–2138.

Sasaki T, Yamamoto Y, Ezaki B, Katsuhara M, Ahn SJ, Ryan PR, Delhaize E, Matsumoto

H. 2004. A wheat gene encoding an aluminum-activated malate transporter. The Plant Journal **37**(5), 645–653.

Sawaki Y, Iuchi S, Kobayashi Y, *et al.* 2009. STOP1 regulates multiple genes that protect Arabidopsis from proton and aluminum toxicities. Plant Physiology **150**(1), 281–294.

Sawaki Y, Kihara-Doi T, Kobayashi Y, Nishikubo N, Kawazu T, Kobayashi Y, Koyama H, Sato S. 2013. Characterization of Al-responsive citrate excretion and citrate-transporting MATEs in *Eucalyptus camaldulensis*. Planta **237**(4), 979–989.

Stack JH, DeWald DB, Takegawa K, Emr SD. 1995. Vesicle-mediated protein transport: regulatory interactions between the Vps15 protein kinase and the Vps34 PtdIns 3-kinase essential for protein sorting to the vacuole in yeast. The Journal of cell biology **129**(2), 321–334.

Takahashi S, Monda K, Higaki T, Hashimoto-Sugimoto M, Negi J, Hasezawa S, Iba K. 2017. Differential Effects of Phosphatidylinositol 4-Kinase (PI4K) and 3-Kinase (PI3K) Inhibitors on Stomatal Responses to Environmental Signals. Frontiers in plant science **8**, 677.

Thompson LA, Ellman JA. 1996. Synthesis and applications of small molecule libraries. Chemical Reviews **96**(1), 555–600.

Tokizawa M, Kobayashi Y, Saito T, Kobayashi M, Iuchi S, Nomoto M, Tada Y, Yamamoto YY, Koyama H. 2015. Sensitive to proton rhizotoxicity1, calmodulin binding transcription activator2, and other transcription factors are involved in aluminum-activated malate transporter1 expression. Plant physiology **167**(3), 991–1003.

Trott O, Olson AJ. 2010. AutoDock Vina: improving the speed and accuracy of docking with a new scoring function, efficient optimization, and multithreading. Journal of Computational Chemistry **31**(2), 455–461.

van der Luit AH, Piatti T, van Doorn A, Musgrave A, Felix G, Boller T, Munnik T. 2000. Elicitation of suspension-cultured tomato cells triggers the formation of phosphatidic acid and diacylglycerol pyrophosphate. Plant physiology **123**(4), 1507–1516.

Vermeer JEM, Thole JM, Goedhart J, Nielsen E, Munnik T, Gadella Jr TW. 2009. Imaging phosphatidylinositol 4-phosphate dynamics in living plant cells. The Plant Journal **57**(2), 356–372.

Walker EH, Pacold M, Perisic O, Stephens L, Hawkins PT, Wymann MP, Williams RL. 2000. Structural determinants of phosphoinositide 3-kinase inhibition by wortmannin, LY294002, quercetin, myricetin, and staurosporine. Molecular Cell **6**(4), 909–919.

Wang CR, Yang AF, Yue GD, Gao Q, Yin HY, Zhang JR. 2008. Enhanced expression of

phospholipase C 1 (*ZmPLC1*) improves drought tolerance in transgenic maize. Planta **227**(5), 1127–1140.

Yang ZB, He C, Ma Y, Herde M, Ding Z. 2017. Jasmonic acid enhances Al-induced root growth inhibition. Plant physiology **173**(2), 1420–1433.

Zabludoff SD, Deng C, Grondine MR, *et al*. 2008. AZD7762, a novel checkpoint kinase inhibitor, drives checkpoint abrogation and potentiates DNA-targeted therapies. Molecular Cancer Therapeutics **7**(9), 2955–2966.

Zheng Z, Amran SI, Thompson PE, Jennings IG. 2011. Isoform-selective inhibition of phosphoinositide 3-kinase: identification of a new region of nonconserved amino acids critical for p110α inhibition. Molecular pharmacology **80**(4), 657–664.